

Rule Learning for Knowledge Graph Reasoning under Agnostic Distribution Shift

Shixuan Liu*, Yue He*, Yunfei Wang, Hao Zou, Haoxiang Cheng, Wenjing Yang,
Peng Cui, *Senior Member, IEEE*, Zhong Liu

Abstract—Knowledge graph (KG) reasoning remains a critical research area focused on inferring missing knowledge by analyzing relationships among observed facts. Despite its success, a key limitation of existing KG reasoning methods is their dependence on the I.I.D assumption. This assumption can easily be violated due to unknown sample selection bias during training or agnostic distribution shifts during testing, significantly compromising model performance and reliability. To facilitate the deployment of KG reasoning in wild environments, this study investigates learning logical rules from KGs affected by unknown selection bias. Additionally, we address test sets with agnostic distribution shifts, formally defining this challenge as out-of-distribution (OOD) KG reasoning—a previously underexplored problem. To solve the issue, we propose the Stable Rule Learning (StableRule) framework, an end-to-end methodology that integrates feature decorrelation with rule learning network, to enhance OOD generalization performance. By leveraging feature decorrelation, the StableRule framework mitigates the adverse effects of covariate shifts arising in OOD scenarios, thereby improving the robustness of the rule learning component in effectively deriving logical rules. Extensive experiments on seven benchmark KGs demonstrate the framework’s superior effectiveness and stability across diverse heterogeneous environments, underscoring its practical significance for real-world applications.

Index Terms—Knowledge Graph Reasoning, Rule Learning, Distribution Shift

1 INTRODUCTION

RECENT decades have witnessed the rapid expansion of knowledge graphs (KGs), including widely used resources such as DBpedia [1] and YAGO [2]. These KGs offer structured representations of real-world knowledge, proving invaluable across diverse domains, including healthcare [3], e-commerce [4], and social analysis [5]. However, recent research has revealed that some common relationships in existing large KGs are deficient at a rate exceeding 70% [6]. To mitigate this limitation and enable the discovery of new knowledge, KG reasoning remains a critical research

focus, aiming to infer missing facts by exploiting observed relational patterns [7].

Currently, three major approaches to KG reasoning exist in the literature. The first is the KG embedding (KGE) method, which encodes entities and relations into a continuous vector space, preserving their semantic similarities as evidenced by structural patterns in the KG [8]. The second paradigm employs graph neural networks (GNNs), utilizing message-passing mechanisms to perform reasoning over the graph structure, thereby facilitating inductive learning of relational dependencies. The third approach is rule-based reasoning, which derives or learns logical rules by analyzing statistical regularities from sampled or exhaustively enumerated rule instances (closed paths) within the training graph. Since these rules explicitly represent relational patterns in KGs, they offer interpretable and precise inference capabilities [9]. These strands have been demonstrated to be effective under the independent and identically distributed (I.I.D.) hypothesis, where the testing and training data are independently sampled from the same distribution.

In practice, this hypothesis may face significant challenges due to distributional shifts in queries. We could formalize KG triplets as (query, answer) pairs, where a query comprises a head entity and a relation, and the answer is the tail entity—with the reasoning objective being to generate accurate answers for given queries. The query shift under discussion arises when the test-time query distribution diverges from the training distribution due to various influencing factors, such as heterogeneous user needs (e.g., variations across demographics like country or age) or temporal dynamics (e.g., seasonal trends or public events).

Figure 1 presents two representative cases of out-of-distribution (OOD) KG reasoning scenarios. Since most KGE

- Shixuan Liu is with the College of Computer Science and Technology, National University of Defense Technology, Hunan, China. This research was conducted during his doctoral studies at the Laboratory for Big Data and Decision, National University of Defense Technology. E-mail: szftandy@hotmail.com
- Yue He is with the School of Information, Renmin University of China, Beijing, China. E-mail: hy865865@gmail.com
- Yunfei Wang is with the National Key Laboratory of Information Systems Engineering, National University of Defense Technology, Hunan, China. E-mail: wangyunfei@nudt.edu.cn
- Hao Zou and Peng Cui are with the Department of Computer Science and Technology, Tsinghua University, Beijing, China. E-mail: ahio@163.com, cuiip@tsinghua.edu.cn
- Haoxiang Cheng and Zhong Liu are with the Laboratory for Big Data and Decision, National University of Defense Technology, Hunan, China. E-mail: hx_cheng@nudt.edu.cn, liuzhong@nudt.edu.cn
- Wenjing Yang is with the Department of Intelligent Data Science, College of Computer Science and Technology, National University of Defense Technology, Hunan, China. E-mail: wenjing.yang@nudt.edu.cn

*These authors contributed equally.

(Corresponding authors: Wenjing Yang, Peng Cui.)

This work has been submitted to the IEEE for possible publication. Copyright may be transferred without notice, after which this version may no longer be accessible.

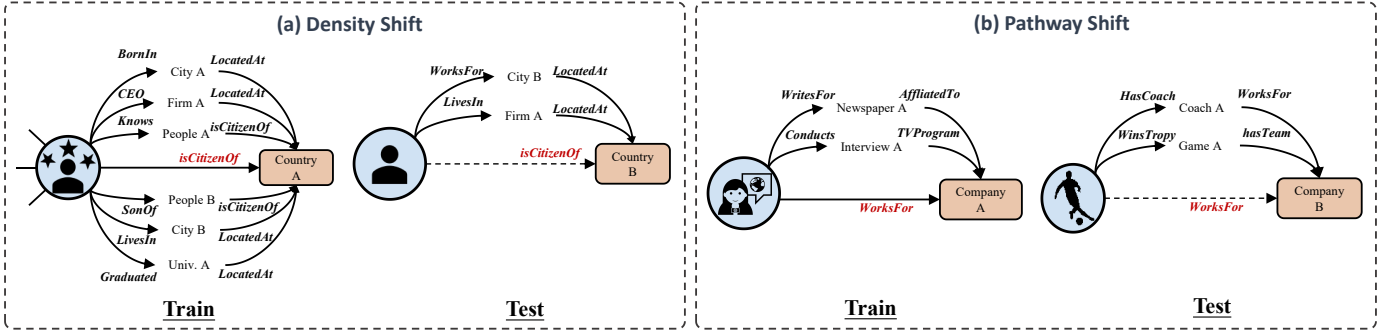


Figure 1. Illustration of KG Reasoning under Query Shift. Solid edges denote observed facts in the training graph, while dashed edges represent target relations to be inferred during testing. (a) Density Shift: Disparity in subgraph density between queried entities. (b) Pathway Shift: compositional reasoning paths scarcely observed during training.

methods are inherently transductive and thus inapplicable to inductive settings with unseen entities, we restrict our analysis to cases where test entities are present in the training graph. The first example, termed the **density shift** scenario (Figure 1(a)), demonstrates an imbalance in subgraph density between the queried entities and the correct answer. While the training set primarily contains facts about high-profile public figures, the test set involves nationality queries concerning the general population. The disproportionate media coverage of celebrities results in substantially more KG facts about these entities, yielding richer evidence and larger subgraph for nationality inference. The second example, termed **pathway shift**, captures a divergence in reasoning patterns between the queried entities and their answers (see Figure 1 (b)). Specifically, the training data consists mainly of journalists, whereas test queries primarily involve footballers. When learning to predict the *WorksFor* relation in the training graph, models are exposed to a high frequency of journalism-related facts (e.g., writing for newspapers, conducting interviews), which may not generalize to footballer-centric test queries.

These distribution shifts pose significant challenges to existing KG reasoning methods. Under density shift, KGE models exhibit a representational bias toward information-rich entities (receiving denser training representations), leading to degraded inference performance on sparsely represented entities [10]. Besides, current GNN-based KG reasoning methods, which largely disregard OOD generalization, struggle with size generalization—particularly when test graphs exhibit substantially different densities [11], [12]. Rule-based methods are similarly vulnerable, as incomplete relation paths in sparse subgraphs undermine inference reliability [13]. For pathway shift, KGE methods, biased toward frequent but domain-specific relation patterns for journalists, fail to generalize to footballer-dominated test data. Standard GNNs, which rely on local subgraph aggregation (e.g., paths or motifs), often learn spurious correlations between structural scaffolds and labels rather than generalizable causal patterns [14], leading to poor test-time performance. Lastly, pathway shift also introduces selection bias in rule instances, favoring journalists over footballers, potentially causing estimation errors in footballer-related rule scores due to rule instances scarcity during training [15].

Although the problem of OOD generalization has been

extensively studied in domains such as regression [16], natural language processing [17], and computer vision [18], it remains largely unexplored in KG reasoning. This gap exists primarily due to the non-Euclidean nature of relational KG data, which requires unique reasoning models with varying representation patterns. Consequently, conventional OOD generalization algorithms—designed to learn $P(Y|X)$ on Euclidean data $\{(X, Y)\}$ —cannot be directly applied.

Notably, recent data-driven rule learning methods have established a representation-based framework that models rule plausibility through conditional distributions $P(r_h|\mathbf{r}_b)$, leveraging semantic consistency from observed rule samples $\{(\mathbf{r}_b, r_h)\}$ [19]. Building on insights from OOD research, we identify that covariate shift in the relation path distribution $P(\mathbf{r}_b)$ introduces estimation errors in plausibility score like $P(r_h|\mathbf{r}_b)$. Our empirical analysis also confirms the presence of selection bias in $P(\mathbf{r}_b)$. Since path distributions encode fundamental topological properties of KGs [20], analysis over $P(\mathbf{r}_b)$ helps gauge distributional shifts and may facilitate the characterization of other sources of shifts in KG reasoning. Given above observations, we aim to mitigate covariate shift in $P(\mathbf{r}_b)$.

Parallel to such development, stable learning has emerged as a scalable alternative to conventional OOD methods, enabling robust performance under distribution shift and broad utility without requiring domain labels. Motivated by these two complementary advances, we investigate how to learn logical rules from KGs with selection bias, for reasoning on test triples with agnostic distribution shifts. We assume that test queries are sampled from multiple environments with varying selection biases. Our objective is to ensure that the learned rules generalize effectively across these diverse and potentially unknown environments, thereby enhancing the stability and robustness of KG reasoning performance.

To achieve above objective, we propose Stable Rule Learning (StableRule), a novel framework comprising two key components: a feature decorrelation regularizer and a rule learning network. First, a backtracking-enhanced rule sampler uniformly draws rule instances across all relations, enabling efficient exploration of potential rule bodies. The rule learning network, which parameterize the plausibility score, then processes these instances using an encoder to map rule bodies into latent embeddings, followed by a

decoder that predicts the rule head from these embeddings. Concurrently, the feature decorrelation regularizer computes weights for each rule body embedding. These weights mitigate correlations among embedding variables by reweighting the training samples. The weighted embeddings are subsequently integrated into the prediction loss function, promoting the learning of generalizable rule patterns.

Main contributions in this paper are as below:

- To the best of our knowledge, we are the first to investigate logical rule learning under OOD KG reasoning scenario, addressing agnostic distribution shifts in KG test sets.
- We propose StableRule, an end-to-end framework that integrates feature decorrelation with an encoder-decoder rule learning architecture. By incorporating reweighting mechanisms, our approach effectively eliminates spurious feature correlations.
- Through extensive experiments on seven benchmark KGs, we demonstrate that StableRule achieves competitive performance with SOTA KG reasoning methods, exhibiting favorable effectiveness and generalization capability across diverse environments.

The remainder of this paper is organized as follows. Section 2 provides a systematic review of related works. Section 3 formally defines our problem setting and analyses the OOD problem to motivate our framework. Section 4 present the architecture of our proposed framework. Section 5 demonstrates the empirical results through comprehensive experiments on three critical tasks: statistical relation learning, standard KG completion, and inductive link prediction. Section 6 further investigate the properties of StableRule, including model convergence behavior, rule interpretation, visualization of feature decorrelation effects, and ablation studies. Finally, Section 7 concludes with key findings and directions for future research.

2 RELATED WORK

2.1 Knowledge Graph Reasoning

In KG reasoning, structure embedding is a well-established approach that map entities and relations onto latent feature spaces considering distance or tensor decomposition. Translation embedding models defines relation-dependent translation scoring functions to measure the likelihood of triples based on distance metrics. TransE [21] is the base translation model that balance effectiveness and efficiency, engendering numerous translation models [22], [23]. RotatE [24], in particular, models each relation as a rotation in the whole complex space, showing impressive representation capacity. Tensor decomposition methods decompose the high-dimensional fact tensor into multiple lower-dimensional matrices for inference, including RESCAL [25], DistMult [26] and ComplEx [27].

Given the graph-structured nature of KGs, GNNs is particularly suitable for KG reasoning. RGCN [28] encodes entities via relation-specific neighborhood aggregation and reconstructs facts using a decoder, but its limited variability in entity representations restricts expressiveness. To address this, M-GNN [29] introduced atten-

tion, while COMPGCN [30] used entity-relation composition operations. Recent GNN-based work explores out-of-KG scenarios, focusing on inductive reasoning for unseen entities, rather than the OOD generalization problem in traditional machine learning. GraIL [31] applies RGCN to local subgraphs for inductive reasoning, while NBFNet [32], A*Net [33], and RED-GNN [34] optimize GNN propagation for efficiency.

Rule-based method is another branch for reasoning over KGs, known for their interpretability and generalizability to unseen entities. These methods originate from inductive logic programming [35], [36], but their scalability remains a challenge due to the NP-hard steps involved [37]. Rule learning methods thus learn rules and weights in a differentiable way. Neural-LP [9] adopts an attention-based controller to score a rule through differentiable tensor multiplication, but could over-estimate scores for meaningless rules. DRUM [38] addresses this by using RNNs to sift out potentially incorrect rule bodies. Since these approach still involve large matrix multiplication, RNNLogic [15] try to solve scalability issue by partitioning rule generation and rule weight learning, but still struggles with KGs with hundred-scale relations or million-scale entities. RLogic [19] thus defines a predicate scoring model trained with sampled rule instances to improve efficiency. NCRL [39] further define the score of a logical rule based on the semantic consistency between rule body and rule head.

None of these methods take the prevalent distribution shifts between the training and testing data into account, an aspect that this paper investigates for the first time.

2.2 Out-of-Distribution Generalization

Domain generalization aims to learn a model using data from a single or multiple interrelated but distinctive source domains, in such a way that the model can generalize well to any OOD target domain. By assuming the heterogeneity of the training data, these methods employ extra environment labels to learn invariant models capable of generalizing to unseen and shifted testing data. Numerous approaches fall under the category of domain alignment, where the primary objective is to reduce the divergence among source domains to learn domain-invariant representations [40], [41], [42], [43], [44], [45]. Some studies expand the available data space by augmenting source domains [46], [47], [48]. Furthermore, a handful of approaches have benefitted from exploiting regularization through meta-learning and invariant risk minimization [49], [50].

Since the presence of correlations among features can disrupt or potentially undermine model predictions, recent studies have centered their efforts on diminishing such correlations during the training process. Some pioneering works theoretically bridge the connections between correlation and model stability under mis-specification, and propose to address such a problem via a sample reweighting scheme [51], [52]. The optimization of the weighted distribution relies on a group of learned sampling weights designed to remove the correlations among covariates. It has been theoretically established that these models can leverage only those variables that encapsulate invariant correlations for predictions [53]. Given such property, these methods are

suitable for addressing the covariate shift problem in a more pragmatic scenarios where only single-source training data is provided [14], [18], [54].

3 PROBLEM DEFINITION AND ANALYSIS

This section establishes the definitions, formalizes the problem, and presents its analysis. For notational consistency, all key terms and symbols are standardized in Table 1.

Table 1
Notation and Definitions.

Notation	Definition
E	Set of entities in the knowledge graph.
R	Set of relations in the knowledge graph.
$G = (E, R, \mathcal{F}_o)$	Knowledge graph subject to reasoning.
$\mathcal{F}_o = \{(q, a)\}$	Set of observed facts used for model training, where each fact could be considered as a query-answer pair.
$\mathcal{F}_u = \{(q', a')\}$	Set of unobserved facts used for evaluation.
$q = (e_h, r, ?)$	A query to be answered involves predicting the tail entity given a head entity and a relation.
$a = (e_t)$	The answer to a query, representing the tail entity e_t .
\mathbf{q}'_m	Query set in the m -th test environment.
M	Total number of distinct test environments.
\mathbf{r}_b	Rule body, defined as a conjunction of relations.
r_h	Rule head, denoting a target relation to be inferred.
$S(\mathbf{r}_b, r_h)$	Plausibility score assigned to the rule (\mathbf{r}_b, r_h) .
N	Batch size for rule samples during training.
d	Embedding dimensionality for rule bodies.
\mathbf{Z}_{n*}	Embedding representation of the n -th rule body
\mathbf{Z}_{*i}	The random variable in the i -th dimension.
$\mathbf{W} = \{w_n\}_{n=1}^N$	The weights associated with the rule samples, where w_n is the weight for the n -th rule sample

3.1 Rule Learning Task

This subsection formally defines the rule learning task, adapting notation to precisely characterize OOD rule learning task, which will be formally introduced in the next subsection.

Definition 1 (Knowledge Graph Reasoning). A KG is formally defined as a structured representation $G = \{E, R, \mathcal{F}_o\}$, where E represents the set of entities, R denotes the set of relations, and \mathcal{F}_o comprises the set of observed facts. Each fact in \mathcal{F}_o is expressed as a triple (e_h, r, e_t) , where $e_h, e_t \in E$ and $r \in R$. Alternatively, facts can be interpreted as query-answer pairs (q, a) , where the query takes the form $q = (e_h, r, ?)$ and the answer is $a = e_t$.

The primary objective of KG reasoning is to model the conditional distribution $P(a|G, q)$ for inferring answers to queries. During testing, KG reasoning models are assessed on a set of unobserved test facts $\mathcal{F}_u = \{(q', a')\}$.

Logical rules play a pivotal role in enhancing KG reasoning, as they provide interpretable and logically grounded explanations for predictive tasks. Most rule-based methods focus on learning chain-like compositional Horn rules to facilitate scalable reasoning over KGs. These rules are formally defined as follows:

Definition 2 (Horn Rule). A compositional Horn rule is comprised of a body of conjunctive relations and a head relation, as follows:

$$S(\mathbf{r}_b, r_h) : r_{b_1}(x, z_1) \wedge \cdots \wedge r_{b_l}(z_{l-1}, y) \rightarrow r_h(x, y) \quad (1)$$

where $S(\mathbf{r}_b, r_h) \in [0, 1]$ represents the rule's plausibility score, and the antecedent $r_{b_1}(x, z_1) \wedge \cdots \wedge r_{b_l}(z_{l-1}, y)$ constitutes the **rule body** (a relation path of length l), and the consequent $r_h(x, y)$ denotes the **rule head** (target relation for reasoning).

When variables in such rules are instantiated with concrete entities, we obtain a **rule instance** (alternatively termed a closed path). For notational convenience, we represent rules as $(\mathbf{r}_b, r_h) \in \mathcal{R}$, where $\mathbf{r}_b = [r_{b_1}, \cdots, r_{b_l}]$ compactly encodes the rule body. Given a rule set \mathcal{R} with associated scores, we can efficiently compute candidate answer scores $a' \in \mathcal{E}$ through forward chaining [55] (see Appendix C).

3.2 Rule Learning Task under OOD Setting

Current KG reasoning methods are predominantly evaluated under the assumption that test facts follow the same distribution as training facts, as both sets are typically derived from a single, complete KG via random splitting. This evaluation protocol inherently ensures identical distributions between training and test queries. However, such an assumption may not hold in practical scenarios, where query distributions can shift due to dynamic and diverse user demands. For instance, as illustrated in Section 1, while the training data may contain abundant facts about journalists, the actual reasoning task may primarily involve queries about footballers and their affiliated companies. Such discrepancies represent a form of agnostic shift, where query distribution shifts naturally arise in real-world applications. To rigorously characterize this challenge, we introduce the following definition:

Definition 3 (Out-of-Distribution Knowledge Graph Reasoning). The OOD KG reasoning task involves $\{G, \mathcal{F}_o, \mathcal{F}_u\}$. During training, a model learns the conditional distribution $P(a|G, q)$ from G and $\{(q, a)\} \subseteq \mathcal{F}_o$. At test time, it is evaluated on diverging sets of queries \mathbf{q}'_m drawn from M heterogeneous test environments, i.e., $\mathcal{F}_u = \{(\mathbf{q}'_m, \mathbf{a}'_m)\}_{m=1}^M$. Crucially, for each relation $r \in R$, the distribution of subject entities $P(e_h)$ must vary across test environments to induce meaningful distributional shifts.

The core of OOD KG reasoning lies in systematic shifts in query distributions. For a relation $r \in R$ (e.g., WorksFor), we enforce shifts in $P(e_h)$ across test subgroups—for instance, constructing one group dominated by journalists and another by footballers. Two types of shifts could be naturally considered:

- **Natural Shifts:** Test groups may be partitioned by observable attributes (e.g., professions or nationalities).
- **Synthetic Shifts:** Since exhaustively accounting for exogenous factors is infeasible, an alternative is to classify head entities based on their relation paths to answers.

If a KG reasoning model can effectively learn the conditional probability $P(a|G, q)$ despite variations in query distributions $P(q)$, it should exhibit stability and efficacy across all M heterogeneous environments. To effectively address such an OOD KG reasoning scenario, the objective of our framework is to effectively learn the plausibility score for each rule (\mathbf{r}_b, r_h) in the rule space \mathcal{R} , mitigating

the adverse effects induced by query shifts. Consequently, predictions derived from these scores remain both accurate and stable across diverse environments.

3.3 Problem Analysis

3.3.1 The Impact of Query Shift

As previously discussed, maintaining stable performance under query shifts is our key objective. However, directly measuring performance fluctuations in response to such shifts presents significant methodological challenges. To overcome this, we analyze their effects through the lens of relation path distribution $P(\mathbf{r}_b)$, which fundamentally governs fact inference. This approach captures two critical aspects: (1) selection bias in queried entities modifies both local neighborhood patterns and the global distribution of answer-leading relation paths, and (2) rule-learning methods inherently depend on these head-to-tail connecting paths. We therefore examine the influence of query shift through examination of $P(\mathbf{r}_b)$.

We first analyse the phenomenon of pathway shift caused by query shift, as shown in Figure 1(b). If the training triples contains significantly more journalists than footballers, rule-learning methods will observe a higher frequency of relation paths semantically associated with journalists compared to those associated with footballers. For instance, when reasoning the relation *WritesFor*, rule bodies such as \mathbf{r}_{b1} : *WritesFor* (x, z) \wedge *AffiliatedTo* (z, y) and \mathbf{r}_{b2} : *Conducts* (x, z) \wedge *TVProgram* (z, y) exhibit stronger statistical relevance to journalist head entities. In contrast, \mathbf{r}_{b3} : *HasCoach* (x, z) \wedge *WorksFor* (z, y) and \mathbf{r}_{b4} : *WinsTrophy* (x, z) \wedge *hasTeam* (z, y) are more strongly associated with footballers. Consequently, when the head entity is a journalist, \mathbf{r}_{b1} and \mathbf{r}_{b2} appear more frequently in closed paths obtained through path enumeration than \mathbf{r}_{b3} and \mathbf{r}_{b4} . Thus, in a training graph dominated by journalists, the sampled rule instances will naturally reflect higher marginal probabilities $P(\mathbf{r}_b = \mathbf{r}_{b1})$ and $P(\mathbf{r}_b = \mathbf{r}_{b2})$ compared to $P(\mathbf{r}_b = \mathbf{r}_{b3})$ and $P(\mathbf{r}_b = \mathbf{r}_{b4})$. Reversing the journalist-footballer ratio in the training data would invert this probability distribution. Importantly, footballer-related relations do not disappear entirely from the training graph—their presence remains necessary for learning, albeit in an imbalanced distribution.

Second, we examine the phenomenon of density shift. As depicted in Figure 1(a), this shift occurs when test queries predominantly concern the public, while the rule samples used for training are primarily derived from celebrities. This discrepancy induces a shift in node degree and path sparsity, without necessarily modifying the underlying distribution of relation paths $P(\mathbf{r}_b)$ (though such a change remains highly probable in practice).

The above observations demonstrate that selection bias (or covariate shift) can manifest in the distribution of relation paths $P(\mathbf{r}_b)$, thereby impairing model generalization. Furthermore, the reasoning performance of rule-based models depends heavily on rule quality, as measured by plausibility scores. Therefore, our objective reduces to correcting misjudgments in these plausibility scores induced by selection bias in $P(\mathbf{r}_b)$.

3.3.2 Plausibility Score Selection

Selecting an appropriate plausibility score is critical for rule learning, yet traditional association metrics, such as coverage and confidence, often fail to characterize unknown distribution shifts accurately. We believe an effective score for OOD rule learning should be grounded in representation learning, computationally scalable, and explicitly incorporate relation paths to address these limitations:

Firstly, representation-based scores are particularly valuable for OOD generalization because they extract domain-invariant features robust to distributional shifts. By disentangling high-level semantic patterns from low-level relational combinations, such representations enhance generalization where raw features may lack discriminative power. Besides, scalability is equally essential, especially when query shift happens in large-scale KGs where rule space risk combinatorial explosion. In IID settings, the rule space is often constrained to patterns seen during training, making scalability less critical. However, under covariate shift, models may need to explore a broader rule space (e.g., longer or more complex paths). Lastly, embedding relation paths into the score’s definition enables direct integration with existing OOD algorithms designed to mitigate covariate shift.

With above instructions in mind, we note that recent data-driven approaches could formalize this intuition by constructing plausibility scores from the semantic consistency of rule instances (\mathbf{r}_b, r_h) . These scores, expressed as $P(r_h|\mathbf{r}_b)$, model the probability of the rule head r_h replacing the rule body \mathbf{r}_b in closed-path samples. This formulation not only supports efficient, high-performance reasoning by incorporating path probabilities $P(\mathbf{r}_b)$ but also aligns with the canonical OOD objective $P(Y|X)$. Consequently, our core challenge further boils down to eliminating estimation errors arising from covariate shifts in relation path distributions \mathbf{r}_b while effectively learning $P(r_h|\mathbf{r}_b)$.

3.3.3 Reducing Covariate Shift

Learning $P(r_h|\mathbf{r}_b)$ becomes fundamentally challenging when facing distributional shifts in $P(\mathbf{r}_b)$. Although balancing query group sizes (e.g., equalizing journalists and footballers) during training could potentially mitigate such shifts, it relies on domain expert explicitly revealing the groups to balance, which is labor-intensive and inefficient. In contrast, stable learning, which can balance all the potential groups and consequently reduce the spurious correlation, becomes a satisfactory alternative strategy.

From a machine learning perspective, when estimating $P(Y|X)$ from samples $\{(X, Y)\}_N$, sample selection bias introduces covariate shifts in $P(X)$, creating spurious correlations in the input space [56], [57]. If representations Z are learned as intermediate features (via X to Z to Y), these covariate shifts propagate to Z . Notably, while feature decorrelation has proven effective for tabular/structured data (where features have fixed semantics), recent work demonstrates that operating on learned representations Z yields superior results for complex modalities like images and graphs [14], [18]. We therefore posit that minimizing statistical dependencies in Z offers a principled approach to reducing these errors [58].

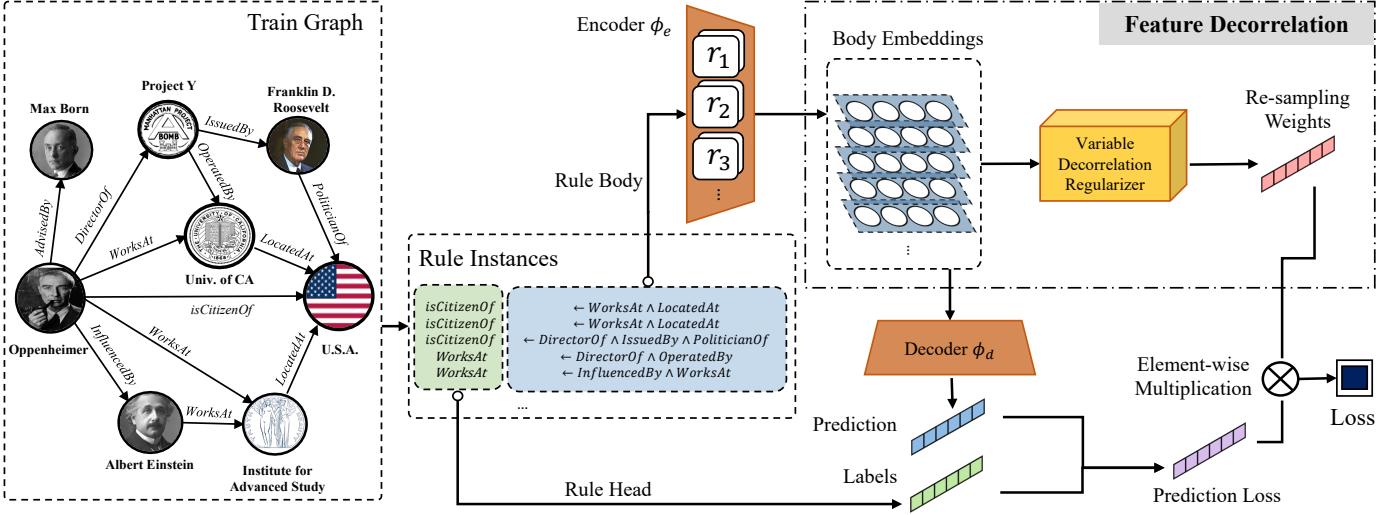


Figure 2. Overview of Methodology. We initially generate a batch of rule instances $\{(\mathbf{r}_b, r_h)\}_N$ from the train graph. The rule bodies are translated into representations with the encoder ϕ_e . Subsequently, the decoder ϕ_d learns to classify these embeddings into corresponding rule heads. To eliminate spurious correlations present in \mathbf{r}_b , we derive a batch of weights \mathbf{W} , with feature decorrelation, to appropriately re-weight the training samples. The overall optimization goal is to minimize the weighted loss.

Under the background of rule learning, where the objective is to learn $P(r_h|\mathbf{r}_b)$, sample bias in $P(\mathbf{r}_b)$ can introduce covariate shifts and spurious correlations in the learned representation $P(\mathbf{Z})$. By eliminating statistical dependencies within $P(\mathbf{Z})$, we could improve the robustness of $P(r_h|\mathbf{r}_b)$ estimation under distribution shifts in $P(\mathbf{r}_b)$. Building on this insight, we propose to use reweighting methods to mitigating covariate shifts in the embedding space $P(\mathbf{Z})$. This approach aligns with stable learning principles, which enhances robustness under distributional shifts by decorrelating input features (or their representations) through reweighting. The reweighting scheme is particularly suitable for our setting because it implicitly handles unknown group structures without manually providing groups for balancing in prior, has been empirically validated for robustness under covariate shifts, and operates flexibly on learned representations to accommodate high-dimensional rule features.

4 METHODOLOGY

This section introduces our proposed StableRule framework, designed to maintain stable reasoning performance under query shifts. The framework’s primary objective is to learn a stable predictor for $P(r_h|\mathbf{r}_b)$ that remains effective even when covariate shifts occur in $P(\mathbf{r}_b)$, thereby supporting reliable KG reasoning under distinct environments.

4.1 Overview

As illustrated in Figure 2, our framework commences with sampling a batch of rule instances $\{(\mathbf{r}_b, r_h)\}_N$ from the training graph, which are subsequently processed by an encoder-decoder framework to parameterize $P(r_h|\mathbf{r}_b)$. The rule encoder, denoted as $\phi_e: \mathcal{R}_b \rightarrow \mathbf{Z}$, maps rule bodies from the input space \mathcal{R}_b to a d -dimensional latent representation space \mathbf{Z} . Conversely, the decoder $\phi_d: \mathbf{Z} \rightarrow \mathcal{R}_h$ reconstructs rule heads from their latent representations.

For a batch of N rule bodies $\{\mathbf{r}_b\}_N$, their corresponding representations are collectively denoted as \mathbf{Z} .

As noted in Section 3.3, a critical challenge arises from covariate shifts in \mathbf{r}_b , which induce covariate shifts in \mathbf{Z} . Specifically, spurious correlations can emerge due to varying dependencies among the covariates of \mathbf{Z} across different environments. To mitigate this bias, we propose a sample re-weighting strategy that enforces statistical independence among the dimensions of \mathbf{Z} . This approach enhances estimation robustness by counteracting the adverse effects of covariate shifts.

Formally, let \mathbf{Z}_{n*} represent the latent embedding of the n -th rule body, and \mathbf{Z}_{*i} denote the random variable associated with the i -th dimension of \mathbf{Z} . The sample weights $\mathbf{W} = \{w_n\}_{n=1}^N$ are constrained such that $\sum_{n=1}^N w_n = N$, where w_n corresponds to the weight assigned to the n -th rule instance $(\mathbf{r}_b, r_h)_n$. Through joint optimization of the encoder ϕ_e , decoder ϕ_d , and sample weights \mathbf{W} , we ensure that the learned representations \mathbf{Z} exhibit minimal statistical dependence across dimensions under the re-weighted distribution. This facilitates the generalization of the composed predictor $\phi_e \circ \phi_d: \mathcal{R}_b \rightarrow \mathcal{R}_h$ to shifted queries.

Since eliminating dependency is the key ingredient for effective rule learning in OOD scenarios, we prioritize the exposition of our methodology for mitigating statistical dependence (Section 4.2) before detailing the parameterization of the rule learning network (Section 4.3) and the overall training scheme (Section 4.4).

4.2 Statistical Independence with Re-weighting

In this subsection, we formalize our approach for achieving statistical independence in the learned representations. Crucially, the intrinsic dependencies within the body representations, particularly between relevant components¹ and

1. The relevant components correspond to discriminative features critical for predicting rule heads, which maintain an invariant relationship with the rule heads under covariate shifts (e.g., semantically-related or synonymous predicates).

irrelevant components², easily lead to the estimation error of $P(r_h|\mathbf{r}_b)$ [50], [59].

When these components exhibit strong interdependencies, they generate spurious correlations that compromise the model's predictive validity. To enable robust prediction of r_h under distributional shifts, our approach systematically eliminates statistical dependencies across all dimensions of the rule body representations. Formally, we implement this via:

$$\mathbf{Z}_{*i} \perp\!\!\!\perp \mathbf{Z}_{*j}, \forall i, j \in [1, d], i \neq j. \quad (2)$$

From [60], we know that \mathbf{Z}_{*i} and \mathbf{Z}_{*j} are independent if,

$$\mathbb{E}[\mathbf{Z}_{*i}^a \mathbf{Z}_{*j}^b] = \mathbb{E}[\mathbf{Z}_{*i}^a] \mathbb{E}[\mathbf{Z}_{*j}^b], \forall a, b \in \mathbb{N} \quad (3)$$

where \mathbf{Z}_{*i}^a represents the element-wise exponentiation of \mathbf{Z}_i raised to the power a . Drawing upon established weighting methodologies in the causal inference literature [61], [62], we propose to enforce statistical independence between \mathbf{Z}_i and \mathbf{Z}_{*j} through sample reweighting using a weight matrix \mathbf{W} . The optimal weights can be derived by minimizing the following objective function:

$$\sum_{a=1}^{\infty} \sum_{b=1}^{\infty} \|\mathbb{E}[\mathbf{Z}_{*i}^a \mathbf{Z}_{*j}^b] - \mathbb{E}[\mathbf{Z}_{*i}^a] \mathbb{E}[\mathbf{Z}_{*j}^b]\|^2 \quad (4)$$

where $\Sigma_{\mathbf{W}} = \text{diag}(w_1, \dots, w_n)$ is the corresponding diagonal matrix. While enforcing exact moment conditions for all variable orders in the objective function (Equation (4)) may be impractical, theoretical insights from [51] demonstrate that reducing first-order moment dependencies can enhance estimation accuracy and model stability. In practice, to balance empirical performance while accounting for potential higher-order correlations in the representation space, we treat the moment order O_d as a hyperparameter in our framework. Consequently, the optimization problem in Equation (4) can be effectively implemented by minimizing the following loss function:

$$L_d = \sum_{i=1}^d \sum_{a=1}^{O_d} \sum_{b=1}^{O_d} \|\mathbf{Z}_{*i}^a \mathbf{Z}_{*i}^b / N - \mathbf{Z}_{*i}^a \mathbf{W} / N * \mathbf{Z}_{*i}^b \mathbf{W} / N\|^2 \quad (5)$$

where \mathbf{Z}_{*i} denotes the complement of the i -th variable in \mathbf{Z}_* , representing all remaining variables when \mathbf{Z}_i is excluded. The summand quantifies the dependence penalty between the target variable \mathbf{Z}_{*i} and its complement \mathbf{Z}_{*i} , capturing their residual statistical association.

Here, we prove that W is learnable and admits at least one solution. While prior work [51] established this result for the special case of first-order moments ($a = b = 1$) in Equation (5), we extend this to arbitrary moment orders.

Lemma 4.1. *If the number of covariates d is fixed, as $h_i \rightarrow 0$ for $i = 1, \dots, d$ and $Nh_1 \dots h_d \rightarrow \infty$, then exists a $W \succeq 0$ such that $\lim_{n \rightarrow \infty} L_d = 0$ with probability 1. In particular, a solution W that satisfies $\lim_{n \rightarrow \infty} L_d = 0$ is $w_n^* = \frac{\prod_{i=1}^d \hat{f}(\mathbf{Z}_{ni})}{\hat{f}(\mathbf{Z}_{n1}, \dots, \mathbf{Z}_{nd})}$, where $\hat{f}(\mathbf{Z}_{*i})$ and $\hat{f}(\mathbf{Z}_{*1}, \dots, \mathbf{Z}_{*d})$ are the Kernel density estimators.*

2. The irrelevant components consist of non-predictive or spurious features, such as noisy relations, redundant semantics without logical dependencies, or coincidental structural patterns (e.g., specific relation path segments) that overfit to training data but lack generalizability.

Proof. From [63], we know if $h_i \rightarrow 0$ for $i = 1, \dots, d$ and $Nh_1 \dots h_d \rightarrow \infty$, $\hat{f}(z_{ni}) = f(z_{ni}) + o_p(1)$ and $\hat{f}(z_{n*}) = f(z_{n*}) + o_p(1)$

Note that for any j, a ,

$$\begin{aligned} 1/N \sum_{n=1}^N \mathbf{Z}_{nj}^a w_n &= 1/N \sum_{n=1}^N \mathbf{Z}_{nj}^a \frac{\prod_{i=1}^d f(\mathbf{Z}_{ni})}{f(\mathbf{Z}_{n1}, \dots, \mathbf{Z}_{nd})} + o_p(1) \\ &= \mathbb{E}[\mathbf{Z}_{nj}^a \frac{\prod_{i=1}^d f(\mathbf{Z}_{ni})}{f(\mathbf{Z}_{n1}, \dots, \mathbf{Z}_{nd})}] + o_p(1) \\ &= \int \dots \int \mathbf{z}_{nj}^a \prod_{i=1}^d f(\mathbf{z}_{ni}) d\mathbf{z}_{n1} \dots d\mathbf{z}_{nd} + o_p(1) \\ &= \int \mathbf{z}_{nj}^a f(z_{nj}) d\mathbf{z}_{nj} + o_p(1) \end{aligned}$$

Similarly, for any k, b ,

$$1/N \sum_{n=1}^N \mathbf{z}_{nk}^b w_n = \int \mathbf{z}_{nk}^b f(z_{nk}) d\mathbf{z}_{nk} + o_p(1)$$

Therefore, for any j and $k, j \neq k$ and any a and b ,

$$\begin{aligned} 1/N \sum_{n=1}^N \mathbf{z}_{nj}^a \mathbf{z}_{nk}^b w_n &= 1/N \sum_{n=1}^N \mathbf{z}_{nj}^a \mathbf{z}_{nk}^b \frac{\prod_{i=1}^d f(\mathbf{Z}_{ni})}{f(\mathbf{Z}_{nj}, \dots, \mathbf{Z}_{nd})} + o_p(1) \\ &= \mathbb{E}[\mathbf{z}_{nj}^a \mathbf{z}_{nk}^b \frac{\prod_{i=1}^d f(\mathbf{Z}_{ni})}{f(\mathbf{Z}_{n1}, \dots, \mathbf{Z}_{nd})}] + o_p(1) \\ &= \int \int \mathbf{z}_{nj}^a \mathbf{z}_{nk}^b f(z_{nj}) f(z_{nk}) d\mathbf{z}_{nj} d\mathbf{z}_{nk} + o_p(1) \\ &= \int \mathbf{z}_{nj}^a f(z_{nj}) d\mathbf{z}_{nj} * \int \mathbf{z}_{nk}^b f(z_{nk}) d\mathbf{z}_{nk} + o_p(1) \end{aligned}$$

Thus,

$$\begin{aligned} \lim_{N \rightarrow \infty} L_d &= \lim_{N \rightarrow \infty} \sum_{a=1}^{O_d} \sum_{b=1}^{O_d} \sum_{j \neq k} (1/N \sum_{n=1}^N \mathbf{z}_{nj}^a \mathbf{z}_{nk}^b w_n - \\ &\quad (1/N \sum_{n=1}^N \mathbf{z}_{nj}^a w_n)(1/N \sum_{n=1}^N \mathbf{z}_{nk}^b w_n))^2 = 0 \end{aligned}$$

□

This theoretical result demonstrates that our proposed variable decorrelation regularizer can effectively decorrelate spurious correlations in \mathbf{Z} by sample reweighting.

4.3 Rule Learning Network

4.3.1 Neural Network Architecture

Various neural architectures can be employed to construct the encoder and decoder for parameterizing $P(r_h|\mathbf{r}_b)$. A critical aspect of this process involves deriving effective embeddings for the input rule body sequence $\mathbf{r}_b = [r_{b1}, \dots, r_{b_l}]$. While traditional sequence models, such as long short-term memory networks (LSTMs) and recurrent neural networks, excel at capturing sequential dependencies, they often fail to model the underlying deductive structure—such as a compositional tree—that governs the derivation of the target relation. To address this limitation, we present an implementation of the encoder-decoder framework that explicitly accounts for the deductive structure. Our design is motivated by the merits of the deductive nature of rules, as further discussed in Appendix D.

Algorithm 1 Stable Rule Learning (StableRule) framework

- 1: **Input:** knowledge graph G and observed facts O .
- 2: Initialize the parameters in the encoder ϕ_e and the decoder ϕ_d for the rule learning network.
- 3: Generate a pool of rule samples with walking strategy described in Section 4.3.2.
- 4: **for** $i = 1$ to T_r **do**
- 5: Sample a batch of rule samples $\{(\mathbf{r}_b, r_h)\}_N$
- 6: Compute body embeddings \mathbf{Z} with $\phi_e(\mathbf{r}_{b,N})$.
- 7: Randomly initialize re-sampling weights \mathbf{W} .
- 8: **for** $j = 1$ to T_d **do**
- 9: Optimize \mathbf{W} by minimizing Equation (5) by rate α_d .
- 10: **end for**
- 11: Optimize ϕ_e, ϕ_d in the direction of Equation (7) with learning rate α_r .
- 12: **end for**
- 13: **Output:** network parameters for ϕ_e and ϕ_d .

The encoder employs a sliding window approach to process relation sequences, where each window of fixed size s at position k is defined as the subsequence $[r_{b_k}, \dots, r_{b_{k+s}}]$. These windows are encoded into continuous representations using an LSTM parameterized by θ : $\Omega_k = \text{LSTM}_\theta([r_{b_k}, \dots, r_{b_{k+s}}])$. The resulting window embeddings Ω are subsequently projected through a fully connected layer to compute a probability distribution Q over the potential logical compositions formed by the windows. This transformation is formulated as $Q = \sigma(W_f \Omega + b_f)$, where $\sigma(\cdot)$ represents the softmax activation function, $W_f \in \mathbb{R}^{1 \times d}$ denotes the weight matrix, and $b_f \in \mathbb{R}$ is the bias term, with d being the window embeddings dimensionality. The window with the maximal probability Q_k is selected for combination. Finally, an attention mechanism is employed to compute a weighted combination of all head relation representations, thereby replacing the original window representation Ω_k by Ω'_k :

$$\Omega'_k = \text{Attention}(\Omega_k) \cdot HW_2 = \sigma\left(\frac{\Omega_k W_1 (HW_2)^T}{\sqrt{d}}\right) HW_2 \quad (6)$$

where, $W_1, W_2 \in \mathbb{R}^{d \times d}$ are trainable weights, and H represent the relation embedding table. Through recursive composition merging over the rule body until convergence to a single window representation, the encoder generates the final body representation \mathbf{Z}_{n^*} . The decoder module share the attention mechanism to compute the head predicate likelihood $P(r_h|Z)$ for each body representation \mathbf{Z}_{n^*} as $\text{Attention}(\mathbf{Z}_{n^*})$.

4.3.2 Backtracking-enhanced Rule Sampling

Rather than exhaustively enumerating all closed paths in the KG, we adopt a path sampling strategy to generate a subset of closed paths as rule instances for model training. To enable efficient sampling, we propose a backtracking-enhanced random walk procedure inspired by principles from stochastic processes [64]. Specifically, the process begins by uniformly sampling a batch of facts $\{(e_h, r, e_t)\}$ for each relation $r \in R$. Then, starting from a source entity e_h , we perform a random walk of fixed length l , where each

subsequent entity e_i is selected based on the transition probability $P(e_i|e_{i-1}) = \frac{1}{|N(e_{i-1})|}$, given that $(e_i, r, e_{i-1}) \in \mathcal{F}_o$.

For the backtracking mechanism, at each step i , we check whether a direct relation exists between the starting entity e_h and the current entity e_i . If such a relation is found, we record the path as a valid rule instance, where the head relation r_h corresponds to the connecting edge and the body \mathbf{r}_b represents the traversed path. Additionally, we incorporate negative sampling by considering non-closed paths. If no relation links e_h and e_i at any point during the walk, we generate a rule sample with r_h labeled as "Neg". This approach ensures an effective exploration of negative rule instances while maintaining computational efficiency.

4.4 Objective Function

Our framework jointly optimizes sample weights \mathbf{W} and the encoder-decoder parameters through an alternating minimization procedure. Unifying the objectives of feature decorrelation and rule learning, we formulate the composite optimization problem as:

$$\hat{\phi}_e, \hat{\phi}_d = \arg \min_{\phi_e, \phi_d} \sum_{i=1}^n w_i L(\phi_d(\phi_e(\mathbf{r}_b^i)), r_h^i) \quad (7)$$

where $L(\cdot, \cdot)$ denotes the cross-entropy loss function. This choice of loss function reflects the rule learning objective, which seeks to maximize the likelihood of the observed target relation in closing the sampled path.

5 EXPERIMENTS

To validate the efficacy of our framework in KG reasoning under agnostic distribution shift, we conduct three key experiments across diverse subgroups: statistical relation learning, standard KG completion (KGC), and inductive link prediction. In statistical relation learning, we assess natural distribution shifts by focusing on reasoning over a single relation. For KGC, we construct synthetic test sets via clustering to ensure query shifts among different test splits. Inductive link prediction follows the same configuration as KGC but operates under a strictly entity-disjoint setting between training and test graphs. The rationale for these experimental designs is elaborated below:

- In statistical relation learning, we focus on reasoning the *Author* relation in the DBLP dataset, which captures paper authorship, to investigate real-world distribution shifts. This setup serves two purposes: (1) examining how an exogenous factor (country) induces natural query shifts and leads to imbalanced model performance across test subgroups, and (2) enabling an in-depth analysis of relation path statistics. Variations in body coverage across subgroups reveal why certain models underperform in specific subgroup.
- KGC serves as a standard benchmark for evaluating KG reasoning methods, requiring models to comprehend all relations and answer to queries involving both $(e_h, r, ?)$ and $(?, r, e_t)$ after a single training phase. To induce systematic query shifts, we generate synthetic test sets through clustering-based partitioning.
- While KGC typically operates in a transductive setting, where distribution shifts may still arise, inductive link

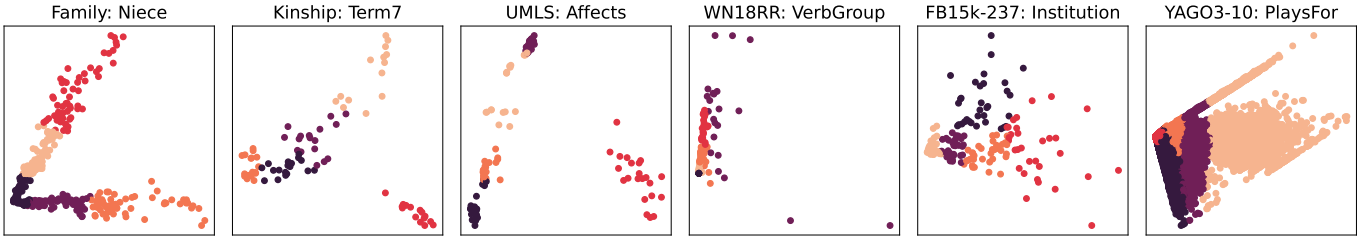


Figure 3. Visualization of the partitioning of test set over one relation. We can see the queries are divided into distinct groups.

prediction enforces entity disjointness between training and test graphs. This setting could better reflect real-world OOD scenarios and often induces more pronounced shifts, as evidenced by observable performance degradation.

Table 2
Statistics of adopted benchmark KGs.

Dataset	# Entities	# Relations	# Facts
Family	3,007	12	28,356
Kinship	104	25	9,587
UMLS	135	46	5,960
WN18RR	40,943	11	93,003
FB15K-237	14,541	237	310,116
YAGO3-10	123,182	37	1,089,040
DBLP	559,396	4	2,381,868

5.1 Experimental Settings

Datasets. To evaluate the effectiveness and robustness of our framework, we conduct experiments on seven widely-used benchmark KGs, including two large-scale datasets. The selected datasets encompass diverse domains and scales: Family [65], Kinship [66], UMLS [66] for smaller-scale evaluation; WN18RR [67], FB15K-237 [68], YAGO3-10 [2] and DBLP [69] for medium to large-scale assessment. Statistics for these datasets are presented in Table 2, while a detailed description of their characteristics and selection rationale is provided in Appendix A.

Utilizing Natural Shift. In statistical relational learning, we introduce a real-world exogenous factor—country affiliation—to partition queries within the DBLP dataset. This approach enables us to examine whether such natural query shifts induce imbalanced model performance across subgroups. Specifically, we evaluate models on their ability to infer authorship for groups of papers where authors are affiliated with different countries. Author country labels are derived using the GeoText package [70], based on the most frequently occurring institutional affiliation for each individual. We restrict our analysis to papers authored by individuals from the top five countries in terms of publication volume (abbreviated as US, CN, DE, FR, and JP).

Creating Synthetic Shift. We utilize the first six datasets to conduct KGC task under synthetic query shifts. To construct test sets that emulate query distribution shifts across different testing environments, we partition the original test set

into five approximately equally sized subgroups. This division is achieved through a controlled clustering procedure applied to the path-describing vector, which quantifies the path counts between each query-answer pair for all possible rule bodies. To ensure a balanced distribution of queries across subgroups for each relation, the clustering operation is performed on a per-relation basis. This approach guarantees distinct query shifts among the test subgroups. The resulting clusters, corresponding to individual relations from each of the six datasets, are visually depicted in Figure 3.

Baselines. We compare our method against 12 competitive approaches, spanning KGE, GNN-based, and rule-learning methods. A comparison of baselines is provided in Table 3, with comprehensive descriptions of them included in Appendix B.

Table 3
Categories of baseline methods

Names	KGE	GNN	Rule Learning
TransE [21]	✓		
DistMult [26]	✓		
Complex [27]	✓		
RotatE [24]	✓		
CompGCN [30]		✓	
NBFNet [32]		✓	
A* Net [33]		✓	
Neural-LP [9]			✓
DRUM [38]			✓
RNNLogic [15]			✓
RLogic [19]			✓
NCRL [39]			✓

Evaluation Metrics. During testing, we evaluate each method by masking either the head or tail entity of every test triple and requiring the model to predict the missing entity. To ensure a rigorous assessment, we employ a filtered evaluation setting and measure performance using three standard metrics: Hit@1, Hit@10, and Mean Reciprocal Rank (MRR). To enhance statistical reliability, we compute the results for each subgroup as the average over five independent runs. The final KG completion performance is then determined by averaging the results across all five subgroups. All reported results are presented in the form of mean \pm standard deviation.

Experimental Setup. Our experiments are conducted on a high-performance computing server equipped with a 64-core CPU, 256 GB of RAM, and eight NVIDIA RTX-3090Ti GPUs, each with 24GB of memory. The proposed

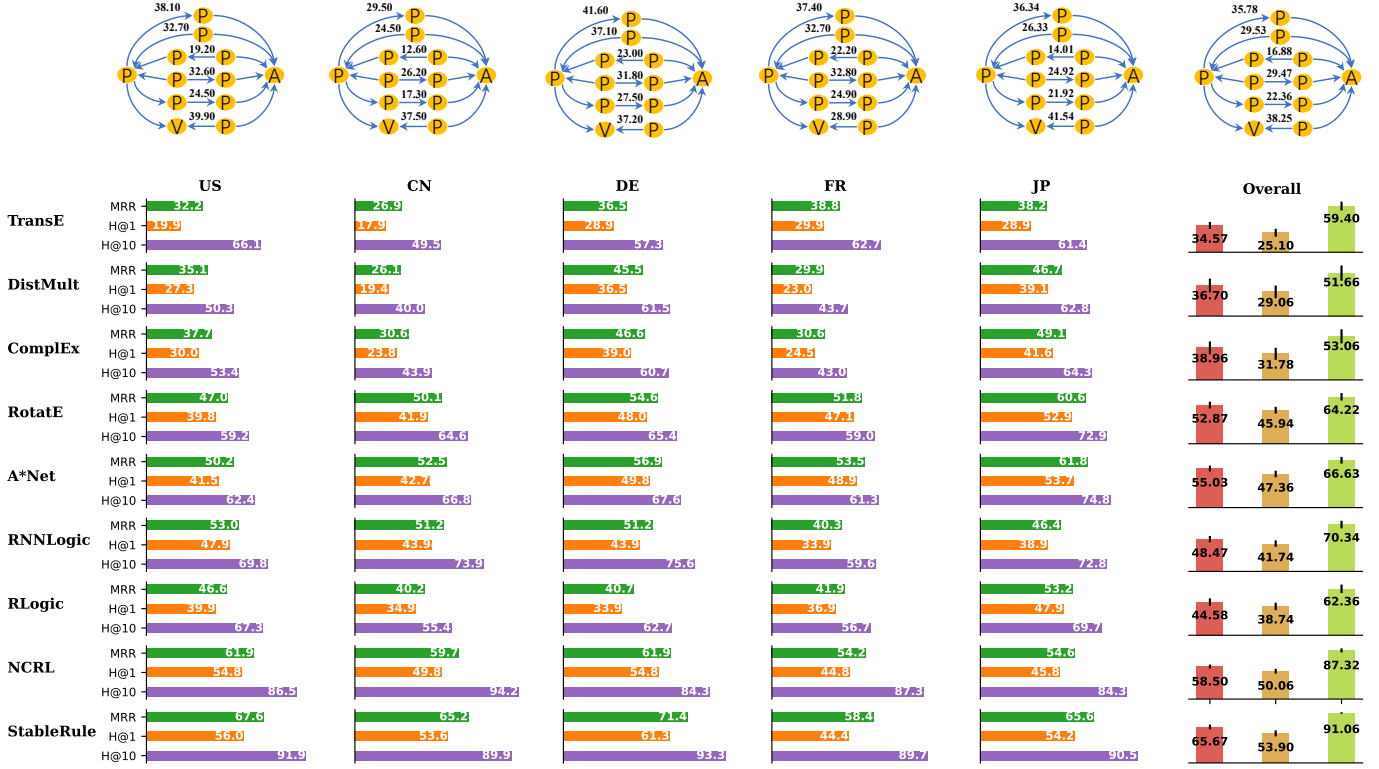


Figure 4. Results on DBLP over subgroups. The above part illustrates the variations in body coverage (which gauges the frequency of each body, shown in %) of selected rules of high confidence, for each respective subgroup and the average population. For example, the 38.10 value (top left) in the US group suggests that 38.10% of Paper-Author pairs are linked through an path instance of Cites (Paper, Paper)\^Author (Paper, Author). Such variation across groups could help explain performance differences. The below part, from left to right, delivers a performance evaluation for each subgroup, followed by the overall performance.

StableRule framework is implemented using PyTorch [71] and trained in an end-to-end fashion. For optimization, we employ the Adam optimizer [72]. The embeddings of all relations are initialized uniformly to ensure consistent starting conditions. To ensure a fair comparison with baseline methods, we determine the optimal hyper-parameters for all competing approaches using a comprehensive grid search strategy. Detailed hyper-parameter configurations for our method are provided in Table 10.

5.2 Statistical Relation Learning

The results for DBLP are presented in Figure 4. As illustrated in Figure 4 (above), a significant disparity in body coverage exists among several top-ranked rules, confirming the presence of selection bias in $P(r_b)$. Furthermore, the findings indicate that path patterns can vary substantially, reflecting differences in research collaboration patterns across the selected countries.

Figure 4 (below) demonstrates that StableRule outperforms all baseline methods, exhibiting a clear performance gap in both effectiveness and stability across all subgroups. KGE models struggle to generate suitable embeddings for all entities within this extensive KG, even after an extended training period of 48 hours. Among GNN-based approaches, while A*Net demonstrates better scalability than NBFNet (which fails to scale entirely), its performance remains suboptimal on this particular dataset. In contrast, other rule-learning models exhibit heightened sensitivity

to shifts in $P(r_b)$ among subgroups, resulting in reduced performance and increased standard deviation.

Notably, each method underperforms in specific subgroups. Our analysis reveals that the worst-case subgroup in terms of MRR consistently corresponds to the CN and FR groups. Further examination indicates significant deviations in path patterns for these groups compared to the average population. These findings reinforce our proposition that developing methods robust to agnostic distribution shifts is critical for improving generalizability.

5.3 Knowledge Graph Completion

The KG completion results are detailed in Table 4. NeuralLP, DRUM, and RNNLogic are unable to accommodate the extensive size of the rule search space on the YAGO3-10 dataset. Evaluating stability in OOD scenarios requires assessing both mean and standard deviation values. It is essential to balance overall effectiveness without disadvantaging lower-performing groups, or conversely, diminishing performance across all groups to reduce variance. The most stable model enjoys enhanced overall performance and small variance.

In comparison to KGE approaches, StableRule demonstrates superior performance over three established KGE models, namely TransE, DistMult, and Complex. Among KGE methods, RotatE emerges as the strongest competitor, maintaining competitive performance across the Family, Kinship, and UMLS datasets. However, this relative advantage decreases with increasing KG scale, since larger KGs

Table 4
Knowledge graph completion results across six datasets, averaged over five sub-populations. Bold and underlined values denote the best-performing results for each dataset among all methods and rule-based methods, respectively.

Methods	Family			Kinship			UMLS		
	MRR (%)	HIT@1 (%)	HIT@10 (%)	MRR (%)	HIT@1 (%)	HIT@10 (%)	MRR (%)	HIT@1 (%)	HIT@10 (%)
TransE	78.05 ±2.29	61.38 ±3.48	97.39 ±1.52	37.68 ±3.46	10.55 ±2.01	85.61 ±5.68	73.86 ±3.34	52.04 ±5.67	98.19 ±0.73
DistMult	66.62 ±3.66	50.99 ±4.47	96.46 ±0.97	41.56 ±2.55	26.48 ±2.49	78.20 ±4.27	57.04 ±4.13	45.98 ±4.59	79.11 ±5.50
CompLex	85.43 ±2.18	76.24 ±2.96	97.99 ±1.24	58.76 ±2.32	45.82 ±2.46	87.35 ±1.94	72.29 ±3.04	57.93 ±3.96	93.92 ±1.90
RotatE	93.85 ±2.36	89.99 ±3.25	99.08 ±1.25	74.50 ±5.15	58.30 ±5.84	96.34 ±3.75	80.24 ±2.08	74.89 ±2.99	97.04 ±0.83
CompGCN	75.35 ±2.90	58.83 ±2.20	88.83 ±2.84	40.30 ±2.63	26.94 ±2.04	75.83 ±3.08	62.33 ±2.23	50.85 ±3.84	72.76 ±1.89
NBFNet	84.16 ±2.00	76.03 ±2.34	97.71 ±0.38	49.54 ±2.78	34.43 ±2.74	81.07 ±2.84	70.74 ±2.43	64.19 ±3.13	82.48 ±1.46
A*Net	82.35 ±2.69	72.37 ±3.21	96.67 ±1.42	44.36 ±2.79	30.42 ±1.95	77.36 ±2.44	66.37 ±2.04	53.63 ±5.51	78.37 ±1.47
Neural-LP	86.12 ±1.75	79.28 ±3.01	97.53 ±1.41	56.17 ±4.39	41.60 ±4.55	87.34 ±4.60	65.38 ±2.36	50.78 ±3.03	88.07 ±1.37
DRUM	86.83 ±2.17	80.70 ±3.63	98.06 ±1.31	47.02 ±5.08	30.11 ±5.35	83.76 ±4.15	68.88 ±1.40	53.37 ±1.22	92.15 ±1.20
RNNLogic	85.74 ±2.56	76.40 ±2.88	96.18 ±1.20	61.78 ±6.04	45.70 ±6.83	91.26 ±5.24	70.20 ±4.92	58.40 ±5.50	91.04 ±2.51
RLogic	86.08 ±2.71	75.81 ±3.26	97.27 ±1.88	59.70 ±6.51	45.60 ±6.87	89.08 ±5.12	67.74 ±7.17	54.32 ±8.33	92.55 ±3.17
NCRL	87.18 ±1.55	78.07 ±2.89	94.34 ±3.25	64.32 ±7.39	51.39 ±7.94	91.56 ±5.89	74.73 ±3.98	59.84 ±5.44	95.15 ±3.78
StableRule	88.88 ±0.57	81.14 ±1.33	98.27 ±0.49	66.01 ±5.69	52.12 ±6.09	92.14 ±4.62	75.90 ±3.88	62.00 ±5.06	95.52 ±3.91

Methods	WN-18RR			FB15K-237			YAGO3-10		
	MRR (%)	HIT@1 (%)	HIT@10 (%)	MRR (%)	HIT@1 (%)	HIT@10 (%)	MRR (%)	HIT@1 (%)	HIT@10 (%)
TransE	19.05 ±2.08	0.91 ±0.82	45.54 ±6.13	37.40 ±1.63	24.65 ±1.09	61.84 ±2.70	34.42 ±4.13	26.78 ±5.14	56.01 ±4.53
DistMult	37.67 ±2.44	34.06 ±3.26	45.38 ±5.31	35.53 ±1.15	23.93 ±1.24	58.46 ±1.59	27.56 ±3.16	19.54 ±2.56	42.93 ±4.27
CompLex	39.99 ±3.67	36.35 ±3.06	47.15 ±6.89	37.49 ±1.81	26.26 ±1.52	59.67 ±2.64	36.34 ±2.45	27.23 ±2.24	53.86 ±3.44
RotatE	41.17 ±3.99	36.92 ±3.23	49.64 ±7.00	40.40 ±1.99	28.24 ±1.70	63.48 ±2.70	40.41 ±3.87	31.76 ±4.34	56.70 ±3.70
CompGCN	45.32 ±3.45	39.25 ±3.35	54.63 ±4.53	33.74 ±2.03	22.98 ±1.73	52.55 ±2.21	28.43 ±2.12	21.36 ±3.67	47.52 ±3.38
NBFNet	53.87 ±4.75	49.50 ±3.04	62.93 ±4.94	39.22 ±2.33	28.79 ±2.43	57.39 ±3.13	36.83 ±2.31	27.91 ±4.16	55.42 ±3.24
A*Net	51.18 ±4.15	42.82 ±4.45	64.37 ±5.05	39.88 ±2.45	30.89 ±2.76	58.13 ±2.03	36.16 ±4.08	27.36 ±4.31	55.93 ±3.33
Neural-LP	37.67 ±5.34	28.46 ±5.13	56.15 ±5.46	31.45 ±1.53	22.71 ±1.35	48.56 ±1.93	-	-	-
DRUM	37.68 ±5.46	28.41 ±5.28	56.30 ±5.38	31.89 ±1.42	23.17 ±1.28	48.75 ±1.87	-	-	-
RNNLogic	45.28 ±5.35	39.00 ±5.32	55.32 ±5.27	28.59 ±1.65	21.20 ±1.74	45.62 ±1.37	-	-	-
RLogic	46.28 ±6.42	37.64 ±6.08	65.22 ±4.84	29.00 ±2.23	19.78 ±1.93	44.02 ±3.21	35.88 ±4.91	27.22 ±3.24	52.25 ±4.64
NCRL	49.02 ±6.35	41.44 ±7.68	64.79 ±4.41	38.76 ±3.81	29.24 ±3.98	58.46 ±6.68	38.33 ±4.93	29.87 ±5.49	56.14 ±4.68
StableRule	51.01 ±5.97	43.44 ±5.84	65.67 ±4.22	41.16 ±2.42	31.22 ±2.17	61.29 ±3.01	40.26 ±4.29	31.19 ±4.51	57.12 ±3.01

Table 5
Knowledge graph completion results for rule learning methods on FB15K-237 and YAGO3-10 without synthetic shift.

Methods	FB15K-237			YAGO3-10		
	MRR	HIT@1	HIT@10	MRR	HIT@1	HIT@10
Neural-LP	31.56	22.84	49.32	-	-	-
DRUM	31.87	23.29	48.92	-	-	-
RNNLogic	28.67	21.35	45.73	-	-	-
RLogic	29.55	19.87	44.26	36.41	25.87	50.38
NCRL	39.28	29.54	60.06	38.26	29.67	56.16
StableRule	41.45	31.20	61.59	39.89	31.06	57.35

could exhibit higher structural heterogeneity and therefore more frequent distribution shifts. GNN-based approaches, particularly NBFNet and A*Net, demonstrate competitive performance on the WN-18RR dataset, benefiting from their ability to propagate and combine information along relation-conditioned paths. Nevertheless, StableRule outperforms these approaches across the remaining five datasets. When compared with other rule learning methods, StableRule consistently achieves superior performance with evident performance gains. Our model exhibits relatively lower variance, indicating more consistent performance across different data subsets - a characteristic attributable

to its robustness against covariate shift.

Beyond this, we note that KGE methods generally surpass rule-based approaches and typically exhibit smaller standard deviations across diverging subgroups. This advantage stems primarily from their capacity to learn effective entity representations, particularly in smaller-scale. The inherent smoothness of similarity metrics derived from embedding proximity naturally yields lower variance compared to rule-based similarity measures, which are inherently more susceptible to KG incompleteness. However, these strengths are noticeably diminished in inductive scenarios involving unseen entities, which is more pervasive in practical, real-world OOD scenarios.

Although our method is primarily designed for OOD scenarios, it remains effective in the absence of synthetic shifts. As demonstrated in Table 5, while the performance gap between our method and baselines is somewhat reduced compared to the OOD setting, our approach still consistently outperforms NCRL and achieves significantly better results than other rule learning methods. This persistent advantage stems primarily from our decorrelation module’s capability to reduce selection bias inherent in the path sampling process.

Table 6

Inductive link prediction results across three datasets, averaged over five subgroups. Bold and underlined values denote the best results for each dataset among all methods and rule-based methods, respectively.

Methods	WN-18RR			FB15K-237			YAGO3-10		
	MRR (%)	HIT@1 (%)	HIT@10 (%)	MRR (%)	HIT@1 (%)	HIT@10 (%)	MRR (%)	HIT@1 (%)	HIT@10 (%)
KGEs									
NBFNet	52.96 ± 4.43	48.63 ± 3.25	61.39 ± 4.11	37.91 ± 1.89	26.36 ± 2.98	56.47 ± 3.77	36.15 ± 2.13	26.28 ± 2.98	56.47 ± 3.77
A*Net	50.88 ± 3.88	42.33 ± 3.06	63.79 ± 4.00	37.33 ± 1.93	26.02 ± 2.74	57.05 ± 2.99	34.86 ± 2.78	25.75 ± 2.77	55.33 ± 3.12
Neural-LP	24.14 ± 2.34	19.86 ± 2.57	35.56 ± 3.82	14.38 ± 1.71	9.10 ± 1.83	29.34 ± 2.13	-	-	-
DRUM	25.58 ± 2.36	21.06 ± 2.42	38.16 ± 3.85	17.25 ± 1.62	11.70 ± 1.72	30.06 ± 2.28	-	-	-
RNNLogic	31.45 ± 3.88	26.00 ± 5.40	45.36 ± 4.73	25.40 ± 1.76	19.40 ± 2.04	40.74 ± 1.83	-	-	-
RLogic	41.06 ± 4.90	37.04 ± 5.54	51.24 ± 4.87	26.15 ± 1.93	19.78 ± 2.37	43.80 ± 3.26	31.29 ± 2.91	23.89 ± 3.32	49.74 ± 2.84
NCRL	45.46 ± 5.57	39.64 ± 6.24	61.20 ± 4.96	35.53 ± 3.40	26.43 ± 3.38	54.30 ± 4.83	33.61 ± 3.36	27.44 ± 4.40	50.86 ± 3.12
StableRule	48.53 ± 4.25	42.44 ± 4.94	63.68 ± 4.64	38.86 ± 2.57	29.92 ± 3.01	60.08 ± 3.07	38.18 ± 2.57	30.09 ± 2.83	56.28 ± 2.54

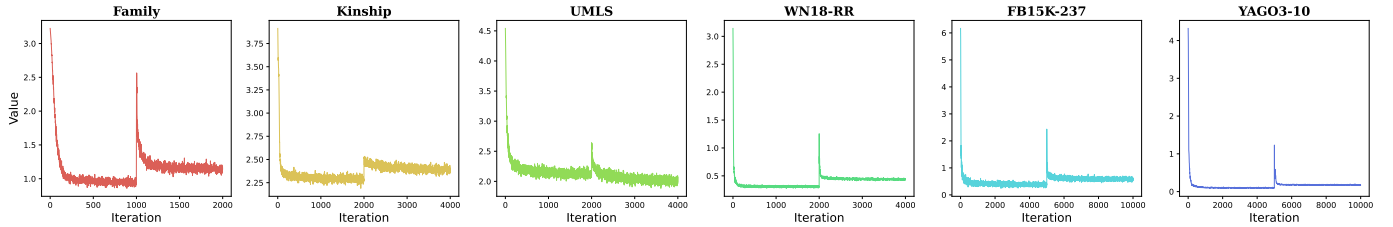


Figure 5. Loss curves on six datasets. Each curve is averaged over 3 runs.

Table 7

Top rules learned by StableRule on YAGO3-10.

$\text{isLocatedIn}(x, y) \leftarrow \text{hasNeighbor}(x, z) \wedge \text{isLocatedIn}(z, y)$
$\text{isLocatedIn}(x, y) \leftarrow \text{hasNeighbor}(x, z_1) \wedge \text{dealsWith}(z_1, z_2) \wedge \text{isLocatedIn}(z_2, y)$
$\text{isCitizenOf}(x, y) \leftarrow \text{isMarriedTo}(x, z) \wedge \text{isCitizenOf}(z, y)$
$\text{isCitizenOf}(x, y) \leftarrow \text{hasAcademicAdvisor}(x, z_1) \wedge \text{worksAt}(z_1, z_2) \wedge \text{isLocatedIn}(z_2, y)$
$\text{livesIn}(x, y) \leftarrow \text{worksAt}(x, z) \wedge \text{isLocatedIn}(z, y)$
$\text{livesIn}(x, y) \leftarrow \text{hasChild}(x, z_1) \wedge \text{isMarriedTo}(z_1, z_2) \wedge \text{livesIn}(z_2, y)$
$\text{graduatedFrom}(x, y) \leftarrow \text{hasAcademicAdvisor}(x, z) \wedge \text{worksAt}(z, y)$
$\text{graduatedFrom}(x, y) \leftarrow \text{hasAcademicAdvisor}(x, z_1) \wedge \text{influences}(z_1, z_2) \wedge \text{graduatedFrom}(z_2, y)$

5.4 Inductive Link Prediction

It should be emphasized that drawing direct comparisons between rule-based methods and KGE methods based solely on transductive completion tasks are inherently inequitable. Unlike KGE approaches, which lack the capability to reason about unseen entities, rule-based methods demonstrate particular strength in inductive scenarios. To construct such inductive scenario, we randomly partitioned all triples in KG into training (70%), validation (10%), and test (20%) sets, ensuring complete entity disjointness between splits. The test set was further divided into subgroups following the aforementioned manner.

Table 6 presents the inductive link prediction results. While GNN-based methods demonstrate relatively smaller performance drops compared to the transductive setting - benefiting from their inherent mechanisms for inductive reasoning - our method still achieves superior performance due to its robust learning capacity. Besides, our analysis reveals that although all rule-based methods exhibit varying degrees of performance degradation in this setting, StableRule exhibited notably stronger performance gap rela-

tive to other rule-based approaches compared to the transductive setting. This enhanced performance gap highlights StableRule’s particular effectiveness in inductive reasoning.

6 FURTHER STUDIES

6.1 Convergence Property

Figure 5 presents the training loss trajectories across all six datasets used in KGC experiments. The observable fluctuations observed during intermediate training stages stem from our sequential rule learning paradigm, wherein the model first acquires 2-length rules before advancing to 3-length rules. Our analysis reveals two significant findings: First, larger batch sizes (corresponding to training on larger knowledge graphs) consistently yield more stable training trajectories with reduced fluctuation magnitudes. Second, all learning curves demonstrate convergence prior to reaching the prescribed iteration limit, with no empirical evidence of improved performance from additional training. This consistent convergence behavior suggests the feasibility of implementing an effective early stopping criterion without compromising model performance.

Table 8
Examining Rules learned by our framework and NCRL

Relation	StableRule	NCRL
isLocatedIn	$\text{hasNeighbor}(x, z) \wedge \text{isLocatedIn}(z, y)$	$\text{isLocatedIn}(x, z) \wedge \text{isLocatedIn}(z, y)$
	$\text{hasNeighbor}(x, z_1) \wedge \text{dealsWith}(z_1, z_2) \wedge \text{isLocatedIn}(z_2, y)$	$\text{hasAcademicAdvisor}(x, z_1) \wedge \text{isLocatedIn}(z_1, z_2) \wedge \text{isLocatedIn}(z_2, y)$
livesIn	$\text{worksAt}(x, z) \wedge \text{isLocatedIn}(z, y)$	$\text{graduatedFrom}(x, z) \wedge \text{isLocatedIn}(z, y)$
	$\text{hasChild}(x, z_1) \wedge \text{isMarriedTo}(z_1, z_2) \wedge \text{livesIn}(z_2, y)$	$\text{hasAcademicAdvisor}(x, z_1) \wedge \text{hasAcademicAdvisor}(z_1, z_2) \wedge \text{livesIn}(z_2, y)$

Table 9
Ablation Results on FB15K-237 and YAGO3-10.

Methods	FB15K-237			YAGO3-10		
	MRR	HIT@1	HIT@10	MRR	HIT@1	HIT@10
StableRule	41.16	31.22	61.29	40.26	31.19	57.12
▷NoDecor	38.91	29.43	59.13	38.29	29.73	56.44
▷FirstMoment	40.37	30.14	59.56	39.40	30.64	56.92
▷NoBack	39.86	29.77	59.24	39.12	30.31	56.83

6.2 Mined Rules

Table 7 presents the logical rules learned by StableRule on the YAGO3-10 dataset. These rules demonstrate both strong interpretability and notable structural diversity, providing comprehensive explanatory coverage for each head relation.

We also carefully compared the rules learned by NCRL and StableRule. Such comparison reveals two key advantages of our approach. First, regarding rule generality, Table 8 shows that while NCRL primarily depends on education-related information for both districts and individuals, our model focuses on more fundamental and invariant properties: neighborhood relationships for districts, and professional and familial connections for individuals. Second, in terms of semantic validity, we observe that NCRL occasionally produces rules with questionable applicability, such as associating the hasAcademicAdvisor relation with districts - a clearly inappropriate linkage that could generate spurious predictions. In contrast, our model consistently generates semantically appropriate rules that properly reflect domain knowledge and entity-relation compatibility.

6.3 Decorrelation Visualization

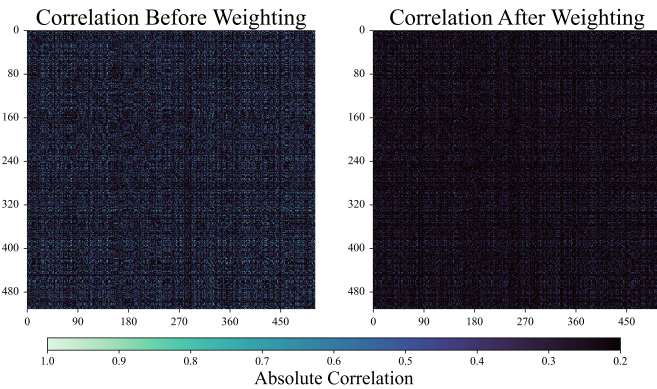


Figure 6. Comparison of feature correlation matrices before (left) and after (right) reweighting. Diagonal elements are set to zero. The reweighted version exhibits reduced inter-feature correlations.

We compare the feature correlation matrices before and after reweighting. To isolate inter-feature correlations, we explicitly zero out the diagonal elements, as self-correlations are uninformative for measuring independence. As shown in Figure 6, the left image (before decorrelation) exhibits distinct banded and grid-like correlation patterns, whereas the right image (after decorrelation) appears nearly blank, with significantly reduced values. This visual result demonstrates that our decorrelation module successfully removes spurious feature correlations through optimized sample reweighting, and thereby support the effective learning of plausibility scores.

6.4 Ablation Studies

Since our model integrates feature decorrelation and rule learning within a unified framework, this section presents ablation studies to assess the utility and sensitivity of its key components and design choices. We specifically analyze three aspects: (1) feature decorrelation (where we term the framework variant without this component as NoDecor), (2) higher-order correlation elimination (with the variant that only reduces first-order moment dependencies termed FirstMoment), and (3) the backtracking mechanism generates more rule instances (with the variant lacking this component termed NoBack). These three configurations are empirically evaluated on both the FB15K-237 and YAGO3-10 datasets.

The results presented in Table 9 demonstrate several important findings. First, removing feature decorrelation leads to an average 5.18% decrease in MRR performance, validating the significance of this regularization component. Second, while reducing only first-order dependencies yields better results than complete removal of the regularizer, this FirstMoment variant still underperforms compared to the full model. Finally, disabling the backtracking mechanism results in an average 2.99% MRR reduction, indicating that sampling more diverse rule instances contributes to mitigating distribution shift.

7 CONCLUSION

In this work, we investigate the challenge of learning logical rules for knowledge graph reasoning under agnostic distribution shifts. We propose a stable rule learning framework comprising two key components: (1) a feature decorrelation regularizer and (2) a rule-learning network. Our novel approach employs a re-weighting mechanism designed to decorrelate rule body embeddings, effectively addressing the covariate shift problem induced by query distribution shifts. Comprehensive experiments across diverse reasoning scenarios demonstrate the efficacy of our method.

Our ongoing research will pursue three key directions: First, we aim to further reduce both linear and non-linear statistical dependencies in embeddings through Random Fourier Feature analysis. Second, we intend to systematically investigate additional sources of distribution shifts and develop corresponding mitigation strategies. Finally, we will explore the development of stable embedding-based models for handling agnostic distribution shifts, potentially trading some interpretability for enhanced and sustained performance.

ACKNOWLEDGMENTS

This work was supported in part by the National Natural Science Foundation of China (NSFC, 62372459, 62206303, 62001495), China. We would like to express our gratitude to Haotian Wang and Renzhe Xu for their valuable advices.

REFERENCES

- [1] S. Auer, C. Bizer, G. Kobilarov, J. Lehmann, R. Cyganiak, and Z. Ives, "Dbpedia: A nucleus for a web of open data," in *The semantic web*. Springer, 2007, pp. 722–735.
- [2] F. M. Suchanek, G. Kasneci, and G. Weikum, "Yago: a core of semantic knowledge," in *Proceedings of the 16th international conference on World Wide Web*, 2007, pp. 697–706.
- [3] Y. Zhang, M. Sheng, R. Zhou, Y. Wang, G. Han, H. Zhang, C. Xing, and J. Dong, "Hkgb: an inclusive, extensible, intelligent, semi-auto-constructed knowledge graph framework for healthcare with clinicians' expertise incorporated," *Information Processing & Management*, vol. 57, no. 6, p. 102324, 2020.
- [4] X. Wang, X. He, Y. Cao, M. Liu, and T.-S. Chua, "Kgat: Knowledge graph attention network for recommendation," in *Proceedings of the 25th ACM SIGKDD international conference on knowledge discovery & data mining*, 2019, pp. 950–958.
- [5] B. Abu-Salih, M. Al-Tawil, I. Aljarah, H. Faris, P. Wongthongtham, K. Y. Chan, and A. Beheshti, "Relational learning analysis of social politics using knowledge graph embedding," *Data Mining and Knowledge Discovery*, vol. 35, no. 4, pp. 1497–1536, 2021.
- [6] T. Shen, F. Zhang, and J. Cheng, "A comprehensive overview of knowledge graph completion," *Knowledge-Based Systems*, p. 109597, 2022.
- [7] X. Chen, S. Jia, and Y. Xiang, "A review: Knowledge reasoning over knowledge graph," *Expert Systems with Applications*, vol. 141, p. 112948, 2020.
- [8] Y. Dai, S. Wang, N. N. Xiong, and W. Guo, "A survey on knowledge graph embedding: Approaches, applications and benchmarks," *Electronics*, vol. 9, no. 5, p. 750, 2020.
- [9] F. Yang, Z. Yang, and W. W. Cohen, "Differentiable learning of logical rules for knowledge base reasoning," *Advances in neural information processing systems*, vol. 30, 2017.
- [10] J. Pujara, E. Augustine, and L. Getoor, "Sparsity and noise: Where knowledge graph embeddings fall short," in *Proceedings of the 2017 conference on empirical methods in natural language processing*, 2017, pp. 1751–1756.
- [11] G. Yehudai, E. Fetaya, E. Meir, G. Chechik, and H. Maron, "From local structures to size generalization in graph neural networks," in *International Conference on Machine Learning*. PMLR, 2021, pp. 11975–11986.
- [12] B. Bevilacqua, Y. Zhou, and B. Ribeiro, "Size-invariant graph representations for graph classification extrapolations," in *International Conference on Machine Learning*. PMLR, 2021, pp. 837–851.
- [13] K. Cheng and Y. Sun, "Logical rule learning," *Knowledge Graph Reasoning: A Neuro-Symbolic Perspective*, pp. 107–147, 2024.
- [14] H. Li, X. Wang, Z. Zhang, and W. Zhu, "Ood-gnn: Out-of-distribution generalized graph neural network," *IEEE Transactions on Knowledge and Data Engineering*, 2022.
- [15] M. Qu, J. Chen, L.-P. Xhonneux, Y. Bengio, and J. Tang, "Rnnlogic: Learning logic rules for reasoning on knowledge graphs," in *International Conference on Learning Representations*, 2020.
- [16] S. Levine, A. Kumar, G. Tucker, and J. Fu, "Offline reinforcement learning: Tutorial, review, and perspectives on open problems," *arXiv preprint arXiv:2005.01643*, 2020.
- [17] D. Hendrycks, X. Liu, E. Wallace, A. Dziedzic, R. Krishnan, and D. Song, "Pretrained transformers improve out-of-distribution robustness," *arXiv preprint arXiv:2004.06100*, 2020.
- [18] X. Zhang, P. Cui, R. Xu, L. Zhou, Y. He, and Z. Shen, "Deep stable learning for out-of-distribution generalization," in *Proceedings of the IEEE/CVF Conference on Computer Vision and Pattern Recognition*, 2021, pp. 5372–5382.
- [19] K. Cheng, J. Liu, W. Wang, and Y. Sun, "Rlogic: Recursive logical rule learning from knowledge graphs," in *Proceedings of the 28th ACM SIGKDD Conference on Knowledge Discovery and Data Mining*, 2022, pp. 179–189.
- [20] I. Tishby, O. Biham, R. Kühn, and E. Katzav, "The mean and variance of the distribution of shortest path lengths of random regular graphs," *Journal of Physics A: Mathematical and Theoretical*, vol. 55, no. 26, p. 265005, 2022.
- [21] A. Bordes, N. Usunier, A. Garcia-Duran, J. Weston, and O. Yakhnenko, "Translating embeddings for modeling multi-relational data," *Advances in neural information processing systems*, vol. 26, 2013.
- [22] Z. Wang, J. Zhang, J. Feng, and Z. Chen, "Knowledge graph embedding by translating on hyperplanes," in *Proceedings of the AAAI conference on artificial intelligence*, vol. 28, no. 1, 2014.
- [23] Y. Lin, Z. Liu, M. Sun, Y. Liu, and X. Zhu, "Learning entity and relation embeddings for knowledge graph completion," in *Proceedings of the AAAI conference on artificial intelligence*, vol. 29, no. 1, 2015.
- [24] Z. Sun, Z.-H. Deng, J.-Y. Nie, and J. Tang, "Rotate: Knowledge graph embedding by relational rotation in complex space," *arXiv preprint arXiv:1902.10197*, 2019.
- [25] M. Nickel, V. Tresp, H.-P. Kriegel et al., "A three-way model for collective learning on multi-relational data." in *ICML*, vol. 11, no. 10.5555, 2011, pp. 3 104 482–3 104 584.
- [26] B. Yang, W.-t. Yih, X. He, J. Gao, and L. Deng, "Embedding entities and relations for learning and inference in knowledge bases," *arXiv preprint arXiv:1412.6575*, 2014.
- [27] T. Trouillon, J. Welbl, S. Riedel, É. Gaussier, and G. Bouchard, "Complex embeddings for simple link prediction," in *International conference on machine learning*. PMLR, 2016, pp. 2071–2080.
- [28] M. Schlichtkrull, T. N. Kipf, P. Bloem, R. Van Den Berg, I. Titov, and M. Welling, "Modeling relational data with graph convolutional networks," in *The semantic web: 15th international conference, ESWC 2018, Heraklion, Crete, Greece, June 3–7, 2018, proceedings 15*. Springer, 2018, pp. 593–607.
- [29] Z. Wang, Z. Ren, C. He, P. Zhang, and Y. Hu, "Robust embedding with multi-level structures for link prediction." in *IJCAI*, 2019, pp. 5240–5246.
- [30] S. Vashishth, S. Sanyal, V. Nitin, and P. Talukdar, "Composition-based multi-relational graph convolutional networks," in *International Conference on Learning Representations*.
- [31] K. Teru, E. Denis, and W. Hamilton, "Inductive relation prediction by subgraph reasoning," in *International Conference on Machine Learning*. PMLR, 2020, pp. 9448–9457.
- [32] Z. Zhu, Z. Zhang, L.-P. Xhonneux, and J. Tang, "Neural bellmanford networks: A general graph neural network framework for link prediction," *Advances in neural information processing systems*, vol. 34, pp. 29 476–29 490, 2021.
- [33] Z. Zhu, X. Yuan, M. Galkin, L.-P. Xhonneux, M. Zhang, M. Gazeau, and J. Tang, "A* net: A scalable path-based reasoning approach for knowledge graphs," *Advances in Neural Information Processing Systems*, vol. 36, pp. 59 323–59 336, 2023.
- [34] Y. Zhang and Q. Yao, "Knowledge graph reasoning with relational digraph," in *Proceedings of the ACM web conference 2022*, 2022, pp. 912–924.
- [35] S. Muggleton and L. De Raedt, "Inductive logic programming: Theory and methods," *The Journal of Logic Programming*, vol. 19, pp. 629–679, 1994.
- [36] S. H. Muggleton, C. Feng et al., *Efficient induction of logic programs*. Turing Institute, 1990.
- [37] T. Rocktäschel and S. Riedel, "End-to-end differentiable proving," *Advances in neural information processing systems*, vol. 30, 2017.
- [38] A. Sadeghian, M. Armandpour, P. Ding, and D. Z. Wang, "Drum: End-to-end differentiable rule mining on knowledge graphs," *Advances in Neural Information Processing Systems*, vol. 32, pp. 15 347–15 357, 2019.
- [39] K. Cheng, N. Ahmed, and Y. Sun, "Neural compositional rule learning for knowledge graph reasoning," in *The Eleventh International Conference on Learning Representations*, 2022.

- [40] D. Li, Y. Yang, Y.-Z. Song, and T. Hospedales, "Learning to generalize: Meta-learning for domain generalization," in *Proceedings of the AAAI conference on artificial intelligence*, vol. 32, no. 1, 2018.
- [41] H. Li, S. J. Pan, S. Wang, and A. C. Kot, "Domain generalization with adversarial feature learning," in *Proceedings of the IEEE conference on computer vision and pattern recognition*, 2018, pp. 5400–5409.
- [42] Q. Dou, D. Coelho de Castro, K. Kamnitsas, and B. Glocker, "Domain generalization via model-agnostic learning of semantic features," *Advances in neural information processing systems*, vol. 32, 2019.
- [43] S. Hu, K. Zhang, Z. Chen, and L. Chan, "Domain generalization via multidomain discriminant analysis," in *Uncertainty in Artificial Intelligence*. PMLR, 2020, pp. 292–302.
- [44] V. Piratla, P. Netrapalli, and S. Sarawagi, "Efficient domain generalization via common-specific low-rank decomposition," in *International Conference on Machine Learning*. PMLR, 2020, pp. 7728–7738.
- [45] S. Seo, Y. Suh, D. Kim, G. Kim, J. Han, and B. Han, "Learning to optimize domain specific normalization for domain generalization," in *Computer Vision—ECCV 2020: 16th European Conference, Glasgow, UK, August 23–28, 2020, Proceedings, Part XXII 16*. Springer, 2020, pp. 68–83.
- [46] F. M. Carlucci, A. D'Innocente, S. Bucci, B. Caputo, and T. Tommasi, "Domain generalization by solving jigsaw puzzles," in *Proceedings of the IEEE/CVF Conference on Computer Vision and Pattern Recognition*, 2019, pp. 2229–2238.
- [47] S. Shankar, V. Piratla, S. Chakrabarti, S. Chaudhuri, P. Jyothis, and S. Sarawagi, "Generalizing across domains via cross-gradient training," *arXiv preprint arXiv:1804.10745*, 2018.
- [48] R. Volpi, H. Namkoong, O. Sener, J. C. Duchi, V. Murino, and S. Savarese, "Generalizing to unseen domains via adversarial data augmentation," *Advances in neural information processing systems*, vol. 31, 2018.
- [49] D. Li, J. Zhang, Y. Yang, C. Liu, Y.-Z. Song, and T. M. Hospedales, "Episodic training for domain generalization," in *Proceedings of the IEEE/CVF International Conference on Computer Vision*, 2019, pp. 1446–1455.
- [50] M. Arjovsky, L. Bottou, I. Gulrajani, and D. Lopez-Paz, "Invariant risk minimization," *arXiv preprint arXiv:1907.02893*, 2019.
- [51] K. Kuang, R. Xiong, P. Cui, S. Athey, and B. Li, "Stable prediction with model misspecification and agnostic distribution shift," in *Proceedings of the AAAI Conference on Artificial Intelligence*, vol. 34, no. 04, 2020, pp. 4485–4492.
- [52] Z. Shen, P. Cui, T. Zhang, and K. Kunag, "Stable learning via sample reweighting," in *Proceedings of the AAAI Conference on Artificial Intelligence*, vol. 34, no. 04, 2020, pp. 5692–5699.
- [53] R. Xu, P. Cui, Z. Shen, X. Zhang, and T. Zhang, "Why stable learning works? a theory of covariate shift generalization," *arXiv preprint arXiv:2111.02355*, vol. 2, 2021.
- [54] S. Dou, R. Zheng, T. Wu, S. Gao, J. Shan, Q. Zhang, Y. Wu, and X. Huang, "Decorrelate irrelevant, purify relevant: Overcome textual spurious correlations from a feature perspective," *arXiv preprint arXiv:2202.08048*, 2022.
- [55] E. Salvat and M.-L. Mugnier, "Sound and complete forward and backward chainings of graph rules," in *International Conference on Conceptual Structures*. Springer, 1996, pp. 248–262.
- [56] X. Chen, M. Monfort, A. Liu, and B. D. Ziebart, "Robust covariate shift regression," in *Artificial Intelligence and Statistics*. PMLR, 2016, pp. 1270–1279.
- [57] M. Sugiyama, M. Yamada, and M. C. du Plessis, "Learning under nonstationarity: covariate shift and class-balance change," *Wiley Interdisciplinary Reviews: Computational Statistics*, vol. 5, no. 6, pp. 465–477, 2013.
- [58] R. Xu, X. Zhang, Z. Shen, T. Zhang, and P. Cui, "A theoretical analysis on independence-driven importance weighting for covariate-shift generalization," in *International Conference on Machine Learning*. PMLR, 2022, pp. 24803–24829.
- [59] L. Tu, G. Lalwani, S. Gella, and H. He, "An empirical study on robustness to spurious correlations using pre-trained language models," *Transactions of the Association for Computational Linguistics*, vol. 8, pp. 621–633, 2020.
- [60] T. M. Bisgaard and Z. Sasvári, "When does $e(x_k \cdot y_l) = e(x_k) \cdot e(y_l)$ imply independence?" *Statistics & probability letters*, vol. 76, no. 11, pp. 1111–1116, 2006.
- [61] S. Athey, G. W. Imbens, and S. Wager, "Approximate residual balancing: debiased inference of average treatment effects in high dimensions," *Journal of the Royal Statistical Society Series B: Statistical Methodology*, vol. 80, no. 4, pp. 597–623, 2018.
- [62] C. Fong, C. Hazlett, and K. Imai, "Covariate balancing propensity score for a continuous treatment: Application to the efficacy of political advertisements," *The Annals of Applied Statistics*, vol. 12, no. 1, pp. 156–177, 2018.
- [63] M. Hollander, D. A. Wolfe, and E. Chicken, *Nonparametric statistical methods*. John Wiley & Sons, 2013.
- [64] F. Spitzer, *Principles of random walk*. Springer Science & Business Media, 2013, vol. 34.
- [65] G. E. Hinton *et al.*, "Learning distributed representations of concepts," in *Proceedings of the eighth annual conference of the cognitive science society*, vol. 1. Amherst, MA, 1986, p. 12.
- [66] S. Kok and P. Domingos, "Statistical predicate invention," in *Proceedings of the 24th international conference on Machine learning*, 2007, pp. 433–440.
- [67] T. Dettmers, P. Minervini, P. Stenetorp, and S. Riedel, "Convolutional 2d knowledge graph embeddings," in *Proceedings of the AAAI conference on artificial intelligence*, vol. 32, no. 1, 2018.
- [68] K. Toutanova and D. Chen, "Observed versus latent features for knowledge base and text inference," in *Proceedings of the 3rd workshop on continuous vector space models and their compositionality*, 2015, pp. 57–66.
- [69] J. Tang, J. Zhang, L. Yao, J. Li, L. Zhang, and Z. Su, "Arnetminer: extraction and mining of academic social networks," in *Proceedings of the 14th ACM SIGKDD international conference on Knowledge discovery and data mining*, 2008, pp. 990–998.
- [70] X. Chen, D. Wang, and T. Zhao, "Geotext: an intelligent dynamic geometry textbook," *ACM Communications in Computer Algebra*, vol. 46, no. 3/4, pp. 171–175, 2013.
- [71] A. Paszke, S. Gross, F. Massa, A. Lerer, J. Bradbury, G. Chanan, T. Killeen, Z. Lin, N. Gimelshein, L. Antiga *et al.*, "Pytorch: An imperative style, high-performance deep learning library," *Advances in neural information processing systems*, vol. 32, 2019.
- [72] D. P. Kingma and J. Ba, "Adam: A method for stochastic optimization," *arXiv preprint arXiv:1412.6980*, 2014.
- [73] Y. Sun, J. Han, X. Yan, P. S. Yu, and T. Wu, "Heterogeneous information networks: the past, the present, and the future," *Proceedings of the VLDB Endowment*, vol. 15, no. 12, pp. 3807–3811, 2022.



Shixuan Liu received his B.S. and Ph.D. degrees from the National University of Defense Technology, Changsha, China, in 2019 and 2024, respectively. He is also a visiting scholar in the Department of Computer Science and Technology at Tsinghua University, where he has spent two years. He has published over 10 papers in prestigious journals and conferences, including T-PAMI, T-KDE, T-CYB, CIKM and ICDM, focusing on knowledge reasoning and data mining.



Yue He is an Assistant Professor at School of Information, Renmin University of China. He received his Ph.D. in the Department of Computer Science and Technology from Tsinghua University in 2023. His research interests include out-of-distribution generalization, causal structure learning, and graph computing. He has published more than 20 papers in prestigious conferences and journals in machine learning, data mining, and computer vision. He serves as a PC member in many academic conferences, including ICML2024, Neurips2024, UAI2024 and etc.



Yunfei Wang received the B.S. degree in civil engineering from the Hunan University, Changsha, China, in 2020. She is now pursuing the Ph.D degree at the National University of Defense Technology, Changsha, China. Her research interests include auto penetration test, reinforcement learning and cyber-security.



Zhong Liu received the B.S. degree in Physics from Central China Normal University, Wuhan, Hubei, China, in 1990, the M.S. degree in computer software and the Ph.D. degree in management science and engineering both from National University of Defense Technology, Changsha, China, in 1997 and 2000. He is a professor in the College of Systems Engineering, National University of Defense Technology, Changsha, China. His research interests include intelligent information systems, and intelligent decision making.

sion making.



Hao Zou received the B.E. degree and Ph.D. degree from the Department of Computer Science and technology, Tsinghua University respectively in 2018 and 2023. His main research interests including causal inference and counterfactual learning.



Haoxiang Cheng received the B.S. degree in systems engineering from the National University of Defense Technology, Changsha, China, in 2024, where he is currently pursuing the master's degree. His research interests include large language models, and knowledge reasoning.



Wenjing Yang received the PhD degree in multi-scale modelling from Manchester University, Manchester, U.K., in 2014. She is currently a research fellow with the College of Computer Science and Technology, National University of Defense Technology. Her research interests include machine learning, robotics software, high-performance computing and causal inference.



Peng Cui (Member, IEEE) is an Associate Professor with tenure in Tsinghua University. He got his PhD degree from Tsinghua University in 2010. His research interests include causally-regularized machine learning, network representation learning, and social dynamics modeling. He has published more than 100 papers in prestigious conferences and journals in data mining and multimedia. Now his research is sponsored by National Science Foundation of China, Samsung, Tencent, etc. He also serves as guest editor, co-chair, PC member, and reviewer of several high-level international conferences, workshops, and journals.

tor, co-chair, PC member, and reviewer of several high-level international conferences, workshops, and journals.

Table 10
Hyper-parameters

Hyper-parameter	Symbol	Value	Description
Batch Size	N	500 (Family) 1000 (Kinship, UMLS, DBLP) 5000 (WN18-RR, FB15K-237) 8000 (YAGO3-10)	Batch Size for Rule Samples
Rule Length	l	3	Maximum length for Logical Rules
Embedding Size	d	512 (Family, UMLS, DBLP) 1024 (Kinship, WN18-RR, FB15K-237, YAGO3-10)	Dimension of embeddings for relations
Rule Learning Epochs	T_r	1000 (Family) 2000 (Kinship, UMLS, WN18-RR, DBLP) 5000 (FB15K-237, YAGO3-10F)	Overall Training Epochs
Rule Learning Rate	α_r	0.00025 (Kinship, UMLS, YAGO3-10, DBLP) 0.0001 (Family, WN18-RR) 0.0005 (FB15K-237)	Learning rate to optimize Equation (7)
Weight Learning Rate	α_d	0.01	Learning rate to optimize Equation (5)
Weight Learning Epochs	T_d	50 (WN-18RR) 100 (UMLS, FB15K-237, YAGO3-10) 200 (Family, Kinship)	Re-sampling Weights Training Epochs
Weight Learning Order	O_d	2	The order in Equation (5)

**APPENDIX A
DATASET DESCRIPTION**

- **Family** captures family relations among family members [65].
- **Kinship** contains kinship relations among members of the Alyawarra tribe from Central Australia [66]
- **UMLS** originates from the field of bio-medicine. It contains entities that are biomedical concepts, and relations such as treatments and diagnoses [66]
- **WN18RR** is designed to function as a user-friendly dictionary and thesaurus, as well as facilitate automatic text analysis. Its entities correspond to word senses, and relations define lexical connections between them [67].
- **FB15K-237** represents an online collection of structured data extracted from numerous sources, including user-submitted Wiki [68].
- **YAGO3-10** is a subset of YAGO, a large semantic knowledge base, derived from a variety of sources, such as Wikipedia, WordNet, WikiData, GeoNames [2].
- **DBLP** is a citation network dataset is extracted from DBLP, ACM, Microsoft Academic Graph, and other sources, seeking to understand the relations between scientific papers, authors and publishing venues [69]

**APPENDIX B
BASELINE DESCRIPTION**

- **TransE** [21]: A foundational knowledge graph embedding method that represents relations as translations between entities in a low-dimensional space.
- **DistMult** [26]: A bilinear model that captures pairwise interactions between entities using diagonal relation matrices.
- **Complex** [27]: Extends DistMult to complex-valued embeddings to model both symmetric and antisymmetric relations.
- **RotatE** [24]: Represents relations as rotations in complex space to model various relation patterns including composition.

- **CompGCN** [30]: A GNN that jointly embeds nodes and relations using composition operations for neighborhood aggregation.
- **NBFNet** [32]: Generalizes path-based methods by learning to dynamically combine paths for relation prediction.
- **A* Net** [33]: Extends NBFNet with A*-like heuristic search to guide the reasoning process.
- **Neural-LP** [9]: A differentiable approach to learning logical rules using tensor operations.
- **DRUM** [38]: Extends Neural-LP with RNNs to handle long rule chains and prune incorrect rules.
- **RNNLogic** [15]: Uses an RNN-based generator to produce interpretable logical rules separately apart from reasoning.
- **RLogic** [19]: Introduces recursive logical rule learning through predicate representation learning.
- **NCRL** [39]: A neural compositional rule learning method using attention mechanisms for recursive reasoning.

**APPENDIX C
FORWARD CHAINING**

By using rules \mathcal{R} and rule score, the score for each candidate answer $a' \in E$ could be efficiently derived from logical rules with forward chaining after path counting [55]. Thus, the final predicted answer is obtained by selecting the candidate answer with the highest score. With matrix operations, this could be efficiently achieved by,

$$a = \underset{(r_b, r_h) \in \mathcal{R}}{\operatorname{argmax}} \sum s(r_b, r_h) \prod_{r \in r_b} \mathbf{M}_r \mathbf{V}_{e_h} \quad (8)$$

where $\mathbf{M}_r \in \{0, 1\}^{|E| \times |E|}$ describes the entity pairs connected by relation r and \mathbf{V}_{e_h} is the one-hot encoding for the head entity.

APPENDIX D DEDUCTIVE NATURE

Recent studies have emphasized the critical role of deductive reasoning in constructing effective rule body representations. This deductive property fundamentally means that the semantics of a complete logical expression are determined by both the meanings of its constituent atoms and their compositional structure. Furthermore, the order of deduction has been shown to significantly influence the

fusion of neighboring relations within a rule body [19], [73].

The challenge lies in the combinatorial complexity of determining the optimal deduction order. For a rule body $\mathbf{r}_b = [r_{b_1}, \dots, r_{b_l}]$, there exist $\prod_{j=2}^{l-1} \frac{l+j-1}{j}$ possible decomposition paths. Given the prohibitive computational cost of identifying the globally optimal order, a greedy selection strategy that sequentially choose the most promising relation pair at each step is preferable.